ENHANCING NASA SOUNDING ROCKET CAPABILITIES

THROUGH COMPOSITE MATERIAL ADOPTION

by

Robert Henry Burth
B.S. December 2016, Clemson University

A Thesis Submitted to the Faculty of
Old Dominion University in Partial Fulfillment of the
Requirements for the Degree of

MASTER OF SCIENCE

AEROSPACE ENGINEERING

OLD DOMINION UNIVERSITY
October 2025

Approved by:

ABSTRACT

ENHANCING NASA SOUNDING ROCKET CAPABILITIES
THROUGH COMPOSITE MATERIAL ADOPTION
Robert Henry Burth
Old Dominion University, 2025
Director: Dr. Drew Landman

Sounding rockets are a suborbital research platform employed by NASA for heliophysics, astrophysics, and geospace science investigations, and for technology development. They follow semi-parabolic trajectories and are launched using surplus military, and commercial, solid-propellant rocket motors. NASA sounding rocket payloads are comprised of standard, modular subassemblies, designed to perform specific functions critical to achieving mission success criteria.

Since the program's inception, payload length and mass have trended upwards, limiting the capability of the platform to reach exospheric apogees and decreasing the time above critical altitudes to observe solar and celestial targets. To offset this trend, composite materials may be of use in payload and subsystem design to decrease payload mass. This investigation seeks to understand if there is a practical benefit to introducing composite materials on the NSRP by assessing mission specific impacts to those missions conducted in fiscal year 2024.

To accurately estimate the mass of a composites-based payload, a standard subsystem (NIACS) underwent structural reconfiguration. Materials were selected that align with NSRP design, manufacturing, and testing standards. NIACS reconfiguration resulted in a mass reduction of 19.6% which was then applied to the payload system in entirety. Using vehicle performance carpet plots, delta apogee and time above the Kármán line were determined. Performance improvements were then evaluated against that mission's success criteria to determine if that mission would have benefitted from using composite materials. On average, each mission would have gained 59.8 kilometers apogee and 62.9 seconds above the Kármán line. However, only nine of the seventeen missions would have benefitted from these performance improvements. Two of the missions could have used a lower-impulse launch vehicle to achieve mission success. Upleg stability met programmatic criteria; downleg instability and dynamic pressure improved, showing that ballast would not offset the mass reduction of using composite materials. Cost analysis showed that production costs will increase 39%. For the two missions that could have used a lower-impulse launch vehicle, the cost of the launch vehicle would have offset payload production costs.

In summary, composite materials are not recommended for universal use on NASA sounding rocket payloads due to unclear programmatic benefits and added cost. However, they are justified for optical astrophysics and heliophysics missions, high-apogee (exosphere) requirements, or when they reduce payload costs versus higher impulse launch vehicles. Reflown, recoverable subsystems should use composites to enhance apogee and observation time.

TABLE OF CONTENTS

TABLE OF CONTENTS iii
LIST OF TABLES iv
LIST OF FIGURES v
METHODOLOGY 4
NIACS STRUCTURAL RECONFIGURATION 11
TRAJECTORY ANALYSIS 43
RESULTS 51
CONCLUSION 56
REFERENCES 57
VITA 58

LIST OF TABLES

Table 1: NSRP Fiscal Year 2024 Missions 8
Table 2: Measured NIACS Mass Properties 11
Table 3: NIACS Mass Properties Error 11
Table 4: NIACS Bill of Materials 13
Table 5: Vibration Test Levels for New Payload Designs 35
Table 6: Composite-Based NIACS Bill of Materials 41
Table 7: Fiscal Year 2024 Composites-Based Payload Mass 43
Table 8: Trajectory Metrics 45
Table 9: Original NIACS Production Cost 48
Table 10: Composites-Based NIACS Production Cost 50
Table 11: Mission Benefit 54

LIST OF FIGURES

Figure 1: NASA Sounding Rocket Vehicles....1
Figure 2: NIACS Isometric View....5
Figure 3: NIACS Internal Structures....5
Figure 4: Black Brant IX WSMR Carpet Plot....9
Figure 5: Skin....14
Figure 6: Skin Door Doubler....14
Figure 7: Skin Door....14
Figure 8: Electronics Deck....14
Figure 9: GLNMAC Lift Ring....14
Figure 10: TERN Angle Bracket....14
Figure 11: EFS Mounting Plate....15
Figure 12: Frame Top....15
Figure 13: GIPS Distribution Frame....15
Figure 14: GIPS Regulation Frame....15
Figure 15: Driver Board Frame....15
Figure 16: Power Entry Frame....15
Figure 17: ACS Flight Processor Frame....15
Figure 18: TERN NIACS Connector Plate....15
Figure 19: Tank Cradle....15
Figure 20: Tank Manifold....15
Figure 21: Tank Cushion....15
Figure 22: Tank Restraint Clamp....15
Figure 23: Spacer Plate....16
Figure 24: High Pressure Manifold....16
Figure 25: Manifold Spacer....16
Figure 26: Bi-Level Transfer Valve....16
Figure 27: Regulator Support Bracket....16
Figure 28: Regulator Bracket Spacer....16
Figure 29: Main Manifold....16
Figure 30: CONX Manifold Bracket, Right....16
Figure 31: CONS Manifold Bracket, Left....16
Figure 32: Regulator Bracket....16
Figure 33: Universal Umbilical Bracket....16
Figure 34: Umbilical Bracket Assembly....16
Figure 35: Deck Mounting Bracket....17
Figure 36: Pneumatic Umbilical Bracket....17
Figure 37: Transverse Nozzle Block, Right....17
Figure 38: Transverse Nozzle Block, Left....17
Figure 39: Roll Control Block....17
Figure 40: Transducer Mounting Bracket (1)....17
Figure 41: Transducer Mounting Bracket (2)....17
Figure 42: Main Manifold Mounting Block....17
Figure 43: Existing Composite Structure on NSRP Payloads.....18
Figure 44: Radax Joint....21
Figure 45: Filament Winding Mandrel....21
Figure 46: Filament Winding Mandrel Cross-Section....21
Figure 47: Three-Piece Composite Skin Cross Section....22
Figure 48: Skin Mass per Unit Length....23
Figure 49: Avionics Assembly....24
Figure 50: Pneumatics Assembly....25

Figure 51: NIACS Skin Assembly 25
Figure 52: Proposed NIACS Substructure 27
Figure 53: Major Components Mounted on Substructure 27
Figure 54: Internal Substructure Comparison 28
Figure 55: Power System and Avionics Mounted on Substructure 28
Figure 56: Functional Components Mounted on Substructure, Isometric 29
Figure 57: Functional Components Mounted on Substructure, Side Profiles 30
Figure 58: NIACS Subassembly, Isometric 30
Figure 59: Battery Standoff Plate 31
Figure 60: Integrated Substructure Support 32
Figure 61: Electronics Deck and Substructure Support Comparison 32
Figure 62: Skin Assembly Door and Doubler 33
Figure 63: Skin Length Comparison 33
Figure 64: NIACS Skin Mounted Components 34
Figure 65: Substructure Free Body Diagram 36
Figure 66: Substructure Support Free Body Diagram 36
Figure 67: Deck Bracket Free Body Diagram 36
Figure 68: Substructure FEA FOS Color Map 37
Figure 69: Substructure FEA Factor of Safety per Plies 38
Figure 70: Substructure Support FEA FOS Color Map 39
Figure 71: Substructure FEA Factor of Safety per Plies 39
Figure 72: NIACS Hardware and Pneumatic Tubes .... **Error! Bookmark not defined.**
Figure 73: 52.009 AE Carpet Plot Results 44

INTRODUCTION

Sounding rockets are a suborbital research platform employed by the National Aeronautics and Space Administration (NASA) for heliophysics, astrophysics, and geospace science investigations, and for technology development. Sounding rockets are one of several platforms offered through NASA's Heliophysics Low Cost Access to Space (H-LCAS) program. The NASA Sounding Rocket Program (NSRP) is managed by the Sounding Rocket Program Office (SRPO) and implemented through the NASA Sounding Rocket Operations Contract (NSROC). The NSRP conducts an average of twenty missions per fiscal year from global launch sites [1].

The NSRP uses a variety of standardized launch vehicles to propel payloads, equipped with scientific instruments, into specific regions of interest in Earth's atmosphere and the near-Earth space environment, typically the mesosphere, thermosphere, and exosphere. The vehicles may be single or multiple stages and are composed of surplus military, and commercial, solid-propellant rocket motors. The current stable of sounding rocket vehicles offered by the NSRP is shown in Figure 1.

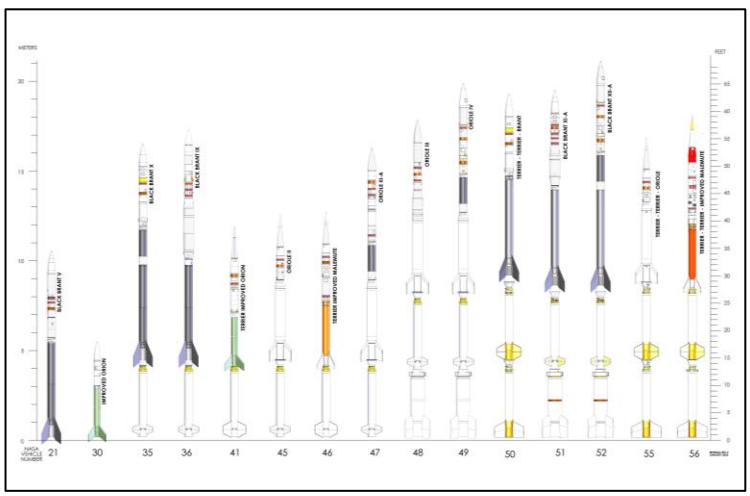

Figure 1: NASA Sounding Rocket Vehicles

Sounding rocket payloads vary in form and function depending on the customer requirements set forth for each mission. Typically, payloads are of three common body diameters, 14 inches, 17.26 inches, or 22 inches. The length of each payload is dependent on the stability of the launch vehicle and the quantity and type of subsystems necessary to conduct the mission. Most payloads are fifteen to twenty-five feet in length from the theoretical nose tip to the motor headcap interface. Common NSRP subsystems include recovery systems, attitude control systems, ignition systems, and boost guidance systems. All payloads include a power and telemetry system that is tailored to the payload instruments, subsystem manifest and for payload housekeeping. Common sounding rocket instruments include telescopes (X-ray, ultraviolet, and optical), magnetometers, particle detectors, and electric field sensors. These instruments are strategically positioned on the sounding rocket payload and are often mounted to dedicated structures for their intended function.

Since the program's inception in 1959, sounding rocket payloads have increased in scale, both in terms of payload gravimetrics (length and mass) and in complexity. While sounding rockets are unique in that payload mass is not directly attributable to launch cost, the increase in payload mass may be indirectly costing NSRP customers opportunity. These opportunity costs include a decrease in time above minimum critical altitudes and the inability to use lower-cost launch vehicles to reach target apogees. The result is often descoping the instrument manifest and using costlier, higher impulse launch vehicles to achieve minimum apogee targets.

NSRP customers and program stakeholders have long understood the limitations of the sounding rocket platform and have sought methods to increase payload performance metrics. For example, in 2000, the Sounding Rocket Working Group (SRWG), an informal committee of active sounding rocket principal investigators, issued a finding to NASA entitled "Maximizing Observing Time". [2] In October of 2009, the SRWG submitted a request to NASA to conduct studies that would increase observation time for astrophysics and heliophysics missions. [3] As recently as 2019, the SRWG communicated the need for "Miniaturization of Sub-systems and Sub-payload development". [4] In this finding, the SRWG emphasized how "lightweight sub-systems could also benefit missions that seek higher apogees, such as those used in the astrophysics and solar communities, as well as geospace payloads that seek the highest altitudes possible…". It is evident that payload mass and length reductions are regularly desired by NSRP customers.

One method to address these findings is to consider alternative materials for the sounding rocket payload. NASA sounding rocket payloads are primarily fabricated from aluminum, including the primary structure, generally referred to as the skin, or what other programs may call a fairing or fuselage. Many internal secondary structures and non-structural parts are also fabricated from aluminum. In some cases, such as when ballast or a stiffer payload is needed for aerodynamic stability, a higher density material, such as steel, is used. A promising alternative to these conventional materials is composite materials as they offer favorable materials properties such as specific weight and specific strength. One disadvantage to composites is increased material cost. As the NSRP is a H-LCAS program element, the increase in material cost may limit its adoption on the program.

There have been studies on how composite materials may be used on the sounding rocket platform [5], but these studies lack institutional knowledge of the NSRP and focus on mass reduction of the skin only. This paper seeks to better quantify the effects of adopting composite materials on the NSRP while providing an accurate cost basis for its implementation. Mass dependent factors such as vehicle stability and whether lower cost launch vehicles are viable for specific missions will also be addressed.

METHODOLOGY

The benefits of incorporating composite materials on the sounding rocket platform must be evaluated relative to mission success criteria on a per mission basis. If there exists no practical benefit to an individual mission, then there is no reason to incorporate composite materials on that mission or the platform in general. Due to the short sounding rocket mission lifecycle, standardized payload configuration design, subsystem design, and part detailed design is required. Programmatically, the design paradigm is to reproduce existing, flight proven designs to decrease design and analysis effort and production costs. Stated differently, part and subsystem designs from payloads that have flight heritage are likely to be reused on future payloads. So, to accurately assess whether incorporating composite materials on the sounding rocket platform is beneficial, programmatic implementation must be considered in addition to the individual mission benefit.

Thus, the approach is to identify standard parts and subsystems currently in use by the NSRP and then consider updating the design of those parts and subsystems to be composites-based. This approach matches NSRP design and manufacturing methodology. The composites-based parts and subassemblies will then be incorporated into existing payload designs to determine how the differences in payload characteristics affect sounding rocket payload performance and contribute to mission success by means of trajectory comparison. A cost-comparison between existing and composites-based designs will be conducted separately.

Using the part and subsystem redesign approach, a standard subsystem which contains stock parts is to be identified. The NSROC provides and supports a variety of subsystems including recovery systems, attitude control systems, and ignition systems. The subsystems are typically self-contained in that they have their own power system, instrumentation, and structures. The subsystem design approach allows for these modules to be interchangeable with one another and to be positioned anywhere in the payload depending on mission specific parameters. Of the systems under consideration, one viable candidate is the NIACS (NSROC Inertial Attitude Control System). The NIACS is an integrated, digital control system whose purpose is to align sounding rocket payloads to inertial targets. [1]. See Figure 2 for an isometric image of the NIACS subsystem, generated in SolidWorks.

Figure 2: NIACS Isometric View

Like other NASA sounding rocket subsystems, the NIACS is self-contained in a skin assembly, its primary structure. There are two internal, secondary structures. The first is the electronics deck which provides mounting features for the avionics, specifically the TERN IMU (Inertial Measurement Unit), GNC Integrated Power System (GIPS), APIF (ACS Processor In Frame), and interface connectors. The second structure is aft of the avionics assembly and supports the pneumatics assembly. The pneumatics assembly structure is a collection of sheet metal and block elements, assembled with fasteners. This structure is not a deck. The pneumatics system is composed of gas tanks, regulators, valves, manifolds, rigid tubes, and associated fittings. These secondary structures and the parts they support are shown in Figure 3.

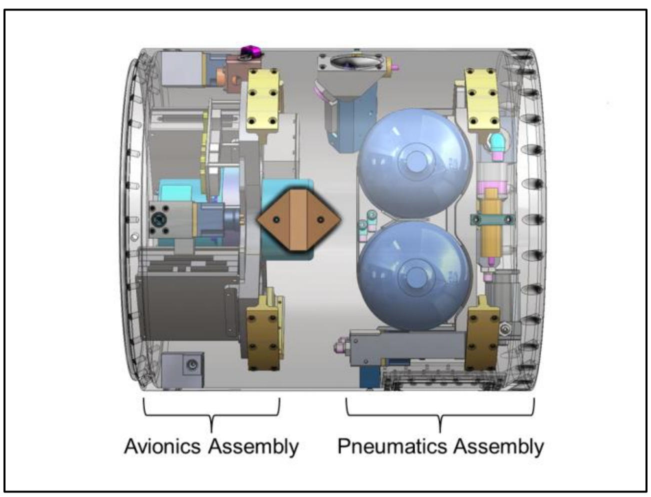

Figure 3: NIACS Internal Structures

There are several nonstructural, skin mounted components including electrical and pneumatic interfaces for payload umbilicals, timer switches, roll and attitude (pitch and yaw) pneumatic blocks, and their associated valves. Most parts in the assembly are manufactured by the NSROC from 6061-T6 aluminum. Select parts and subassemblies (such as the gas tanks, valves, and regulators) are sourced from application specific vendors or are COTS (Commercial Off the Shelf) products. Within the NIACS there are several stock parts commonly used in the design of other payload subsystems. These include the deck mounting bracket, universal umbilical bracket, and pneumatic umbilical bracket. Other parts, though not specifically used elsewhere, are similar in form to other stock parts. For example, the electronics deck is specifically designed for the NIACS, but decks of similar form are used in sounding rocket payload telemetry systems, experiment structures, and in other attitude control systems. The composition of the NIACS is suitable for the objectives of this study as the subsystem design is characteristic of NSRP design practices and contain stock parts found in other sounding rocket payload subsystems.

Before proceeding with NIACS structural reconfiguration, identification of customer needs is essential. By identifying customer needs, a design objective and engineering design requirements for the NIACS reconfiguration process will be established. If adopting composite materials on the sounding rocket platform does not fulfill customer needs, then the change is superfluous.

Primary NASA Sounding Rocket Program customers are principal investigators from university, government, and commercial sectors. Investigations conducted by the NSRP involve “upper atmosphere, plasma physics, solar physics, planetary atmospheres, galactic astronomy, high energy astrophysics and micro-gravity research.” [1] Customer needs vary depending on the type of investigation being conducted and are defined in mission success criteria. These criteria are categorized as either minimum success criteria or comprehensive success criteria. Comprehensive criteria define an ideal, nominal case for payload performance whereas minimum criteria establish a minimum, or off-nominal case, in which the investigation would still be deemed successful by the customer.

Mission success criteria imposed upon the NSRP are typically related to four categories: payload trajectory, payload attitude, instrument function, and subsystem function. Of these categories, payload trajectory and payload attitude will be affected by changing material basis. Instrument and subsystem function will not change. By introducing composite materials to the platform, one seeks to improve payload performance to better meet customer needs.

Some specificity is necessary to better define payload performance relative to payload trajectory and attitude categorization. Having established there being a variety of mission types, each with unique success criteria, there are several underlying performance metrics that may be of some benefit for all missions. Considering payload trajectory, two performance metrics are of interest: payload apogee and payload time above a minimum altitude (or time in environment). Both payload apogee and time above altitude metrics should increase for there to be a benefit to the customer. Considering payload attitude, one performance metric is of interest: time on target. This metric is dependent on the time in environment and payload gravimetrics.

While there are a variety of prospective methods to increase payload apogee, time in environment and time on target, as it relates to composite materials, the clear interest is that of reducing payload mass. By decreasing payload mass, the payload will achieve a higher apogee, be in the environment of interest for longer, and be on target for a greater period of time. Thus, the design objective for the NIACS structural reconfiguration is to minimize the mass of the NIACS without altering its function. This reconfiguration is to be guided by the following, self-imposed, design requirements:

1. The NIACS skin shall retain common joint geometry for the purpose of modularity.
2. The inertial measurement unit shall remain axially aligned with the subsystem thrust axis.
3. Functional elements of the system shall not be altered except for purposes of mounting.
4. Materials are to be ASTM E595 compliant.

These design requirements are necessary to bound the scope of the redesign effort and to ensure compliance to current payload design methods. The first requirement is intended to ensure the redesigned system maintains compatibility with existing sounding rocket subsystems. The skin joint is the only structural interface between sounding rocket subsystems. To introduce a novel joint would disrupt established standards. The approach will be to consider how to fabricate existing joint geometries from composite materials or otherwise maintain the current skin design. The second requirement is intended to maintain the relative position of the IMU on the thrust axis of the payload, to simplify the attitude control system's inertial reference frame. By relocating the TERN IMU to an off-axis position within the NIACS, sensor misalignments are introduced which may affect the absolute pointing accuracy of the onboard instruments. The third requirement is purposed to maintain the function of the NIACS. Functional elements are defined as any part or subassembly which are provided by a vendor (pneumatic regulators, valves, connectors, etc.) or that directly contribute to the function of the NIACS (manifolds and electronics board frames). The fourth requirement is to ensure that the composite materials selected are compliant with the space environment. ASTM E595 is the *Standard Test Method for Total Mass Loss and Collected Volatile Condensable Materials from Outgassing in a Vacuum Environment*. To meet this requirement, only those materials that are commercially available and certified as ASTM E595 will be considered. This will simplify material selection by process of elimination.

Following NIACS structural reconfiguration, payload performance metrics will be estimated and compared against all missions conducted by the NSRP in the 2024 fiscal year. This method is unbiased as the sample size is significant and constitutes a variety of experiment types, launch vehicles, and launch ranges. Annual assessments of the benefit of composite-based payloads will enable program stakeholders to make informed decisions regarding their implementation as the program is funded on an annual basis. The mission manifest for the 2024 fiscal year is taken from the NASA Sounding Rockets Bluebook [6]. Payload mass, apogee, and time above the Kármán Line[1] are taken from program documents, specifically the Mission Readiness Review package. Relevant information is shown in Table *1*.

Mission Number	Experiment Type	Payload Mass $[lb_m]$	Apogee $[km]$	Time Above Kármán Line $[s]$
36.386 UE	Geospace Sciences	977.5	341.3	469.0
36.387 UE	Geospace Sciences	961.4	346.0	473.4
36.388 UE	Geospace Sciences	964.8	344.8	472.3
36.375 UG	UV / Optical Astrophysics	1262.6	261.3	376.7
45.007 GE	Geospace Sciences	1065.6	322.3	448.8
52.009 AE	Geospace Sciences	967.6	472.0	602.1
36.392 UE	Geospace Sciences	677.3	407.6	533.3
36.393 UE	Geospace Sciences	666.2	412.6	537.6
36.394 UE	Geospace Sciences	673.2	409.5	534.9
36.370 US	Solar and Heliospheric	1070.5	262.8	378.7
36.371 NS	Solar and Heliospheric	1183.0	261.1	375.9
36.396 UG	UV / Optical Astrophysics	1104.0	285.6	427.8
41.133 WO	Student Outreach	665.4	119.5	128.7
36.385 NS	Solar and Heliospheric	982.6	338.8	449.2
46.042 WO	Student Outreach	874.0	162.3	231.4
36.384 UG	UV / Optical Astrophysics	1209.6	272.4	396.4
36.366 US	Solar and Heliospheric	1179.4	276.5	394.5

Table 1: NSRP Fiscal Year 2024 Missions

[1]The *Kármán Line* is generally accepted to be 100 km above sea level. The *NASA Sounding Rockets User Handbook* provides standard launch vehicle carpet plots with “Time Above 100 km” data.

To estimate composite-payload performance deltas, it is assumed that the launch vehicle configuration for each mission is unaffected by the change in payload mass properties. This may not be the case in practice. First, rigid rocket stability will be evaluated to determine the impact of composite based payloads on existing launch vehicles configurations. Next, a trajectory will be generated using the mass properties of the composite based payload. To generate a sounding rocket trajectory, the NSROC uses TAOS (Trajectory Analysis and Optimization Software), produced by Sandia National Laboratories. TAOS numerically simulates trajectories using known factors and generates statistical dispersions using bounded offsets and the Monte Carlo method. Such factors include the launch vehicle configuration, launch range, launcher elevation and azimuth, guided rail travel, time of year, payload mass, payload center of gravity, payload moment of inertia, fin count, fin shape, fin angle of attack, ignition delay, etc. While TAOS is the preferred method to generate trajectories for this investigation, it is inaccessible, as are the various factors and offsets.

Without access to TAOS or the requisite factors and offsets, it is impossible to generate trajectories to compare against the original payload trajectory. Analytical, closed-form methods such as using the conservation of energy, conservation of momentum, or equations of motion fail to provide accurate trajectory information. In lieu of this information, estimated apogee deltas and time above the Kármán Line metrics will be taken from carpet plots for each vehicle, as provided in the *NASA Sounding Rockets User Handbook* [1]. One such carpet plot for a 17.26-inch diameter payload launched from WSMR (White Sands Missile Range) on a Black Brant IX is shown in Figure 4. The carpet plot for each vehicle does not account for variations in payload length, time-of-year atmospheres, or other secondary factors so this method's accuracy is limited.

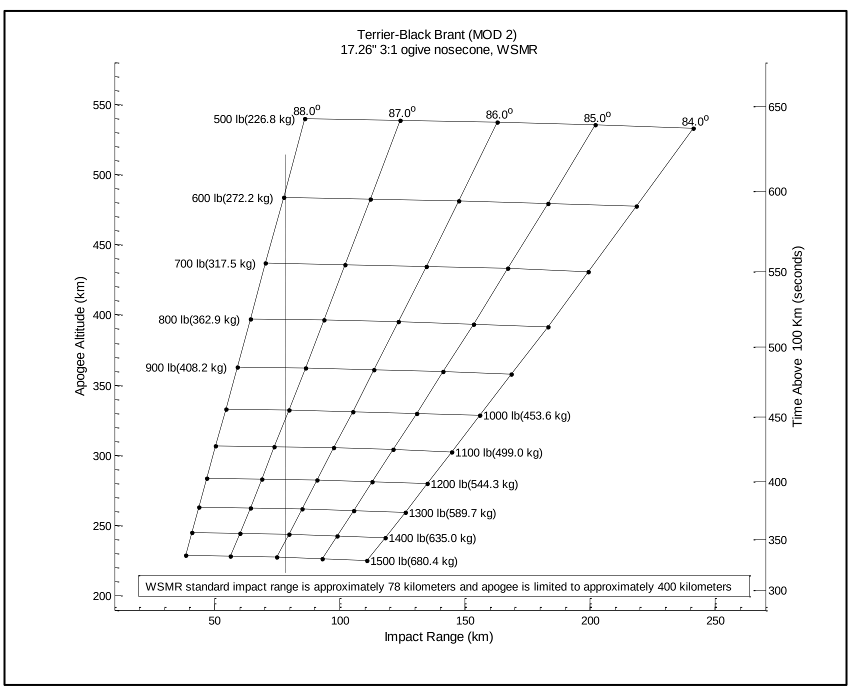

Figure 4: Black Brant IX WSMR Carpet Plot

A cost analysis of the NIACS will also be conducted to understand the difference in manufacturing cost between the original NIACS and a composites-based NIACS. Compared to the 6061-T6 aluminum commonly used for NASA sounding rocket payload components, advanced engineering composites typically have a higher cost per unit mass. As the NSRP is conducted under the H-LCAS program element, cost must be considered. Mission proposals for H-LCAS funding are evaluated based on merit, cost, and relevance [7] so additional costs to individual missions or to the program as a whole limit the effectiveness of the program and the quantity of missions launched on an annual basis.

The cost analysis will include material and labor costs of those parts manufactured by the NSROC or that are unique to either the original NIACS or the composites-based NIACS. The methodology to estimate the cost of the original NIACS will be to use NSROC manufacturing data and vendor provided stock material rates. The approach to estimate the cost of the composites-based NIACS will be to project labor per manufacturing route sheets and vendor provided composite material costs.

The conclusion will incorporate findings on the potential for composite material application in the NSRP, mission specific and programmatic benefits, and estimated recurring production costs. Recommendations and potential secondary effects will be provided, establishing a foundation for future research, trade studies, and potential application.

NIACS STRUCTURAL RECONFIGURATION

The process begins with establishing the specific NIACS subsystem that is undergoing structural reconfiguration. There are multiple skews of the NIACS, the most common being the *NIACS-TG, Bi-Level Short* with two gas tanks, henceforth denoted simply as NIACS. This configuration includes a forward (male) and aft (female) radax joint as the modular subsystem interface. The tanks are filled with an inert propellant gas such as Nitrogen. The directed propulsion from the NIACS is the means by which the system controls the roll rate and attitude of the payload during nonpowered flight. Other configurations of the NIACS have different tank quantities, joints configurations, and nozzle locations. Recall the design objective is to minimize the mass of the NIACS without altering its function. Before reconfiguration commences, the initial mass properties of the system must be established. This particular configuration of the NIACS was selected in part because this system has measured mass properties, given in Table 2.

Length (in)	Weight (lb_f)	Center of Gravity (in)	RMOI $(slug - ft^2)$	PMOI $(slug - ft^2)$
19.50	81.50	9.81	0.68	0.93

Table 2: Measured NIACS Mass Properties

Due to the short design phase of the NASA sounding rocket mission lifecycle, models of payload subsystems lack details that do not directly contribute to the form, fit, or function of the system. Examples of omitted details include fasteners, wire harnesses, pneumatic tubing, and circuit boards. These items are captured in other documentation and are simply absent from the solid model. For this reason, CAD (Computer-Aided Design) estimated mass properties of any subsystem, including the NIACS, are inaccurate. Instead, the NSROC relies on measuring the mass properties of as-built systems, as was done for the NIACS in Table 2. Table 3, reports the estimated mass properties of the NIACS system from SolidWorks. The error compared to the measured system is given in the second row of Table 3 for emphasis.

CAD NIACS Mass Properties	Length (in)	Weight (lb_f)	Center of Gravity (in)	RMOI $(slug - ft^2)$	PMOI[2] $(slug - ft^2)$
	19.50	64.40	9.17	0.78	0.68
Error (%)	0 (0%)	-17.10 (21.0%)	-0.64 (-6.5%)	0.09 (13.6%)	-0.25 (-26.7%)

Table 3: NIACS Mass Properties Error

[2] Sounding rocket payloads are estimated to have equal moments of inertia about in pitch and yaw. The reported PMOI is an average of the pitch moment of inertia and yaw moment of inertia.

Considering the lack of detail in the existing solid body model and lacking the means to manufacture and measure a composites-based NIACS, the level of detail in the redesigned NIACS solid body model will need to exceed that of the original model. The reconfigured NIACS model will need to include all fasteners, pneumatic lines, and fittings. Most electrical parts (wire harnesses, circuit boards, etc.) will be absent as the time needed to accurately model these elements exceed the span of this investigation. The mass contribution of the electrical parts has been determined separately by measuring the mass of an as-build avionics system. The mass of the electrical parts in a NIACS system (not including the IMU) is $4.34\ lb_m$.

Next, an assessment of which parts within the NIACS subassembly may be suitable for redesign is conducted. A Bill of Materials of the original NIACS is shown in Table 4. Parts contained within a subassembly are denoted with detailed numbering. NSROC part numbers have been omitted and some part or subassembly descriptions have been updated for clarity.

Item Number	Description	Quantity (-)	Material	Mass (lb_m)
1	NIACS Skin Assembly	1		
1.1	Skin	1	6061-T6	16.50
1.2	Skin Door Doubler	1	6061-T6	0.44
1.3	Skin Door	1	6061-T6	0.38
2	NIACS Electronic Subassembly	1		
2.1	Electronics Deck	1	6061-T6	6.85
2.2	GLNMAC Lift Ring	1	6061-T6	0.73
2.3	TERN Angle Bracket	4	6061-T6	0.07
2.4	EFS Mounting Plate	4	6061-T6	0.28
2.5	Frame Top	3	6061-T6	0.20
2.6	GIPS Distribution Frame	1	6061-T6	0.16
2.7	GIPS Regulation Frame	1	6061-T6	0.48
2.8	Driver Board Frame	1	6061-T6	0.10
2.9	GIPS Power Entry Frame	1	6061-T6	0.11
2.10	ACS Flight Processor Frame	1	6061-T6	0.91
2.11	TERN NIACS Connector Plate	1	6061-T6	0.11
3	NIACS Pneumatics Subassembly	1		
3.1	Tank Cradle	2	6061-T6	0.93
3.2	Tank Manifold	2	6061-T6	0.15
3.3	Tank Cushion	4	Rubber[3]	0.02
3.4	Tank Restraint Clamp	2	201 SS	0.08
3.5	Spacer Plate	1	6061-T6	0.06
3.6	High Pressure Manifold	1	6061-T6	0.30
3.7	Manifold Spacer	1	6061-T6	0.04
3.8	Bi-Level Transfer Manifold	1	6061-T6	0.65
3.9	Regulator Support Bracket	1	5052-H32	0.30
3.10	Regulator Bracket Spacer	1	6061-T6	0.03
3.11	Main Manifold	1	6061-T6	1.11
3.12	CONX Manifold Bracket, Right	1	6061-T6	0.17
3.13	CONX Manifold Bracket, Left	1	6061-T6	0.18
3.14	Regulator Bracket	1	6061-T6	0.21
4	Umbilical Bracket Assembly	1		
4.1	Universal Umbilical Bracket	1	6061-T6	0.35
4.2	Umbilical Backing Plate	1	6061-T6	0.01
5	Deck Mounting Bracket	8	6061-T6	0.37
6	Pneumatic Umbilical Bracket	1	6061-T6	0.36
7	Transverse Nozzle Block, Right	2	6061-T6	0.56
8	Transverse Nozzle Block, Left	2	6061-T6	0.56
9	Roll Control Block	2	6061-T6	0.57
10	Transducer Mounting Bracket (1)	2	6061-T6	0.02
11	Transducer Mounting Bracket (2)	1	6061-T6	0.02
12	Main Manifold Mounting Block	1	6061-T6	0.14

Table 4: NIACS Bill of Materials

[3] The specific grade of rubber is unspecified. It is assumed to be a 50A durometer polychloroprene (Neoprene).

The Bill of Materials lists only those parts that are designed and fabricated by the NSROC. Parts or subassemblies provided by external vendors such as pneumatic regulators, pneumatic valves, pneumatic fittings, electrical connectors, and circuit boards are outside the scope of this reconfiguration effort. The intent of the structural reconfiguration is to maintain the function of the system by keeping functional components unchanged. Further, pneumatic manifolds and valve blocks are not being considered for material change due to functional and program safety requirements. However, they are included in the Bill of Materials as geometric modifications to the manifolds and valve blocks may be necessary for means of placement and mounting in the new assembly. No fasteners are listed in the Bill of Materials.

The Bill of Materials lists thirty-eight unique parts contained within the parent NIACS assembly. A majority (thirty-six, or ninety-five percent) of the fabricated parts are aluminum, predominantly 6061-T6. The total mass of these components is $41.43\ lb_m$, or fifty-one percent of the NIACS assembly mass. The other $40.07\ lb_m$ are those parts which are functionally dependent. For context of further discussion, isometric images of these parts are provided in Figure 5 through Figure 42. Dimensions are omitted.

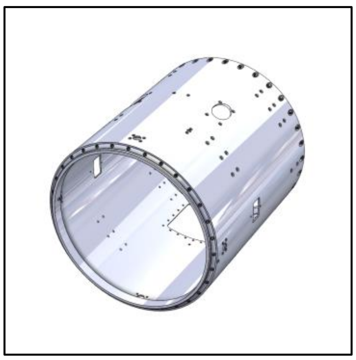

Figure 5: Skin

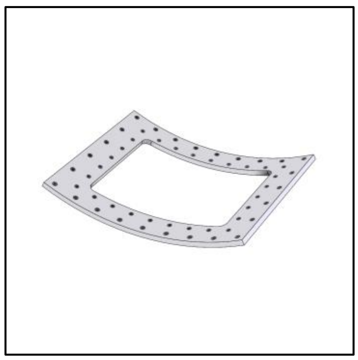

Figure 6: Skin Door Doubler

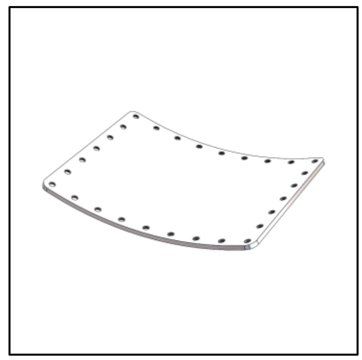

Figure 7: Skin Door

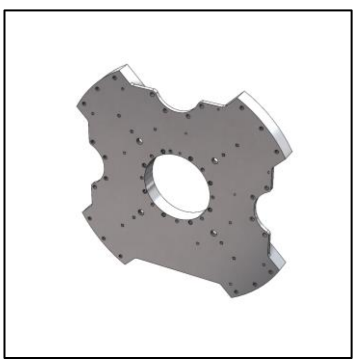

Figure 8: Electronics Deck

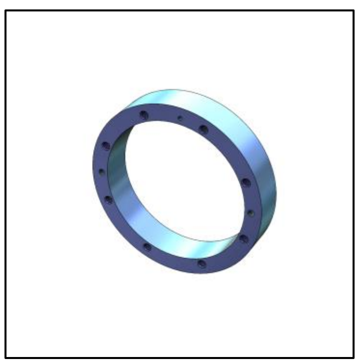

Figure 9: GLNMAC Lift Ring

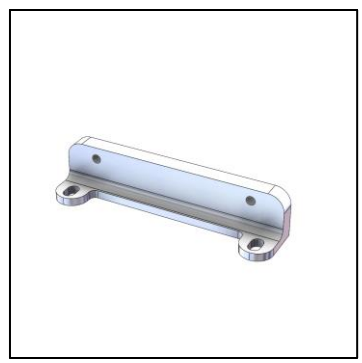

Figure 10: TERN Angle Bracket


Figure 11: EFS Mounting Plate

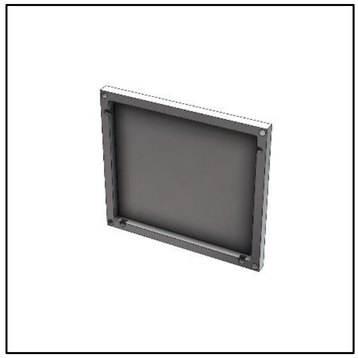
Figure 12: Frame Top


Figure 13: GIPS Distribution Frame

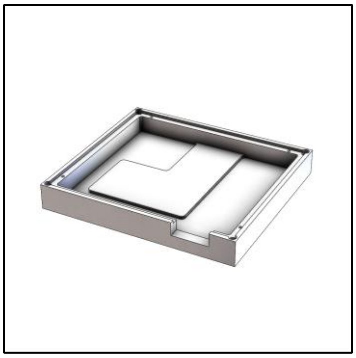
Figure 14: GIPS Regulation Frame


Figure 15: Driver Board Frame


Figure 16: Power Entry Frame

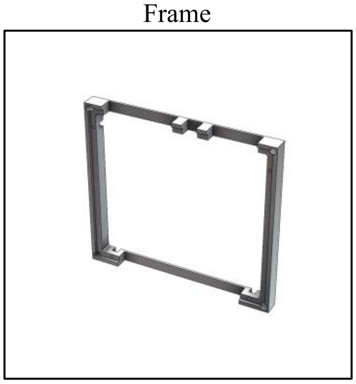
Figure 17: ACS Flight Processor Frame


Figure 18: TERN NIACS Connector Plate


Figure 19: Tank Cradle

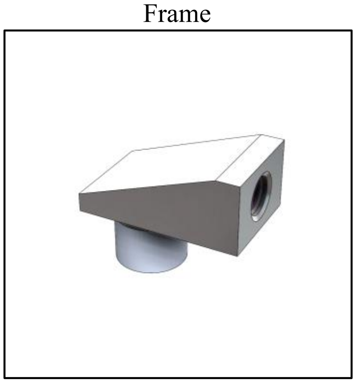
Figure 20: Tank Manifold

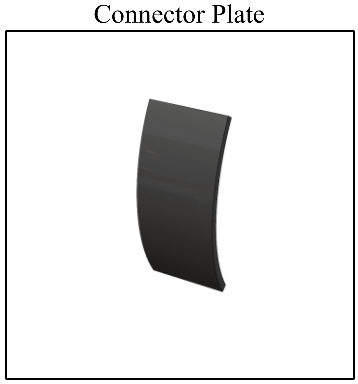
Figure 21: Tank Cushion

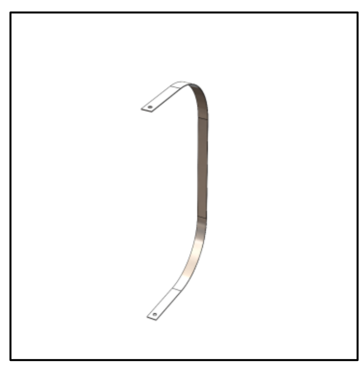
Figure 22: Tank Restraint Clamp

Figure 23: Spacer Plate

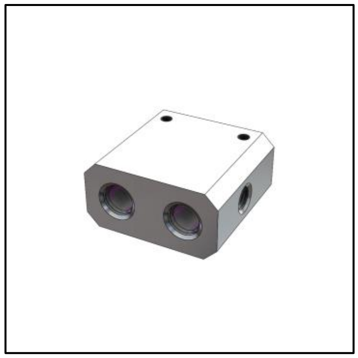

Figure 24: High Pressure Manifold

Figure 25: Manifold Spacer

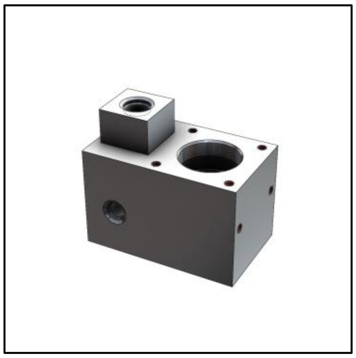

Figure 26: Bi-Level Transfer Valve

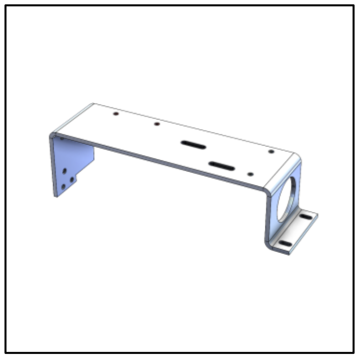

Figure 27: Regulator Support Bracket

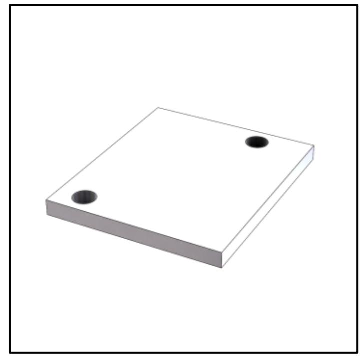

Figure 28: Regulator Bracket Spacer

Figure 29: Main Manifold

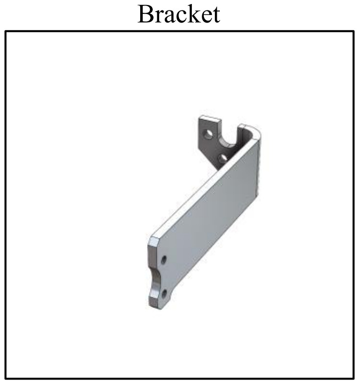

Figure 30: CONX Manifold Bracket, Right

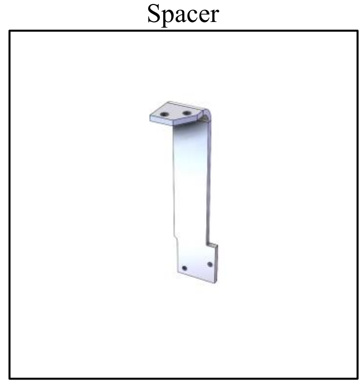

Figure 31: CONS Manifold Bracket, Left

Figure 32: Regulator Bracket

Figure 33: Universal Umbilical Bracket

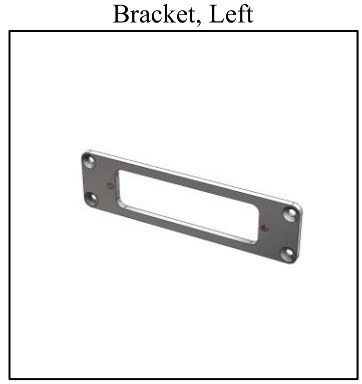

Figure 34: Umbilical Bracket Assembly

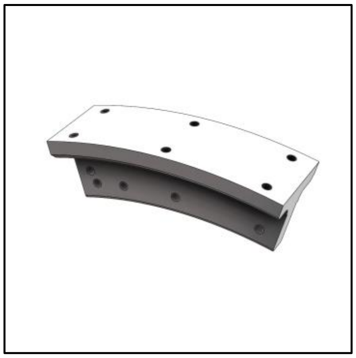

Figure 35: Deck Mounting Bracket

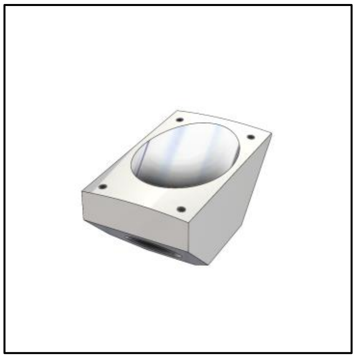

Figure 36: Pneumatic Umbilical Bracket

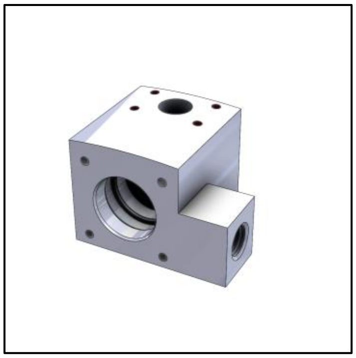

Figure 37: Transverse Nozzle Block, Right

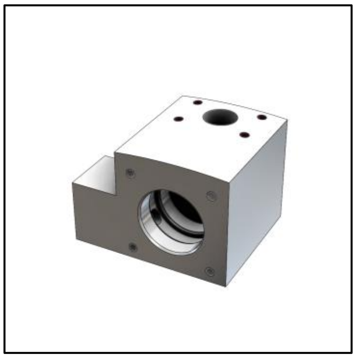

Figure 38: Transverse Nozzle Block, Left

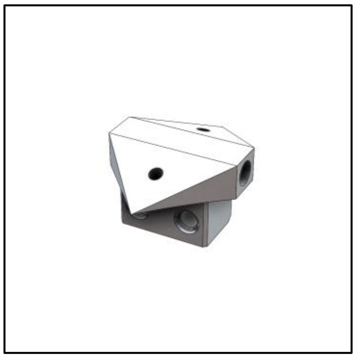

Figure 39: Roll Control Block

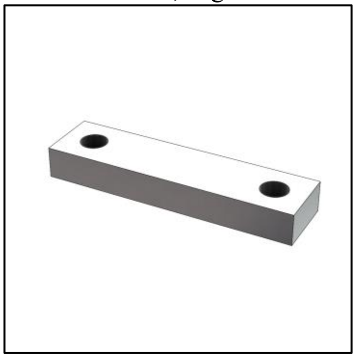

Figure 40: Transducer Mounting Bracket (1)

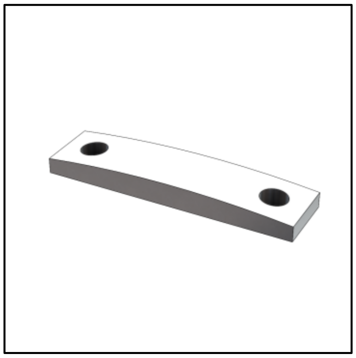

Figure 41: Transducer Mounting Bracket (2)

Figure 42: Main Manifold Mounting Block

Considering the individual components and their forms facilitates an assessment of suitable composite materials and manufacturing processes for the redesigned parts. Concurrent consideration of part geometry and manufacturing processes will ensure parts are designed for manufacturability and align to the short NSRP mission lifecycle.

As identified in Table 4, a majority of sounding rocket payload hardware is conventionally machined from 6061-T6 aluminum. Aluminum is the default material for most payload part hardware because of its low density, high strength, low cost, machinability, availability, and documented material properties. It is also electrically conductive, providing payload and instrument power systems a common chassis ground. Further, it is thermally conductive, allowing high powered electronics, such as transmitters, to dissipate heat into payload structures without dedicated thermal paths. 6061-T6 is also field protective, shielding internal systems that are RFI (Radio Frequency Interference) or EMI (Electromagnetic Interference) sensitive.

There are several direct programmatic and mission lifecycle benefits to using 6061-T6 as the common material for payload hardware that must be considered in the reconfiguration process. The first being decreased material cost due to bulk purchasing of common stock forms. Most parts are fabricated from either sheet, plate, extrusions, or forgings. Minimizing the variety of materials and their stock forms leads to indirect cost savings, including lower procurement and storage expenses. Second, by using 6061-T6 for most parts and considering flight heritage of similarly designed parts, most novel parts designed for a specific mission do not require a structural loading analysis. This is true for a majority of primary structures (payload skins) as well as secondary structures (such as those composed of decks and longerons). By using 6061-T6, a majority of parts are inherently overdesigned and novel designs are justified by comparison. When novel part analysis is required, especially those parts for primary, load-bearing structures or mechanisms, NSRP engineers rely on published material properties, particularly in the MMPDS (Metallic Materials Properties Development and Standardization).

The advantages of using 6061-T6 on the NSRP are rational in its current application. This investigation does not suggest that composites materials should replace all 6061-T6 parts on the payload. There are instances when the function of a part requires a specific material, such as the NIACS pneumatic manifolds. Another example of part function forcing material selection highlights the current application of composite materials on sounding rocket payloads. NASA sounding rockets often manifest magnetometers to measure Earth's magnetic field in situ. Magnetometers and other particle instruments require magnetically clean structures in the vicinity. To fulfill this requirement, the NSRP uses composite substructures, primarily composed of G-10, a glass fiber, epoxy resin, based laminate. An example of such a structure is shown in Figure 43.

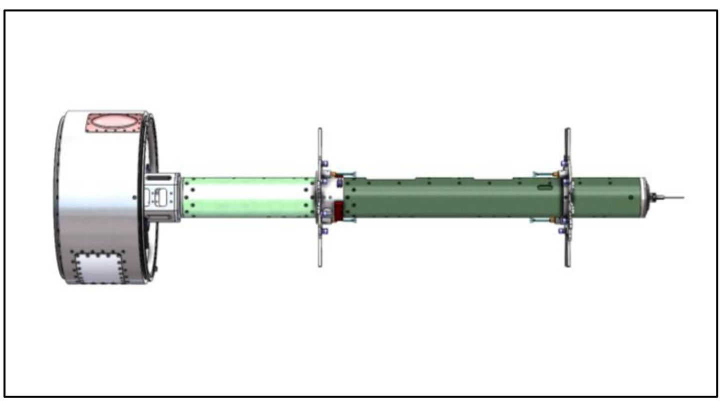

Figure 43: Existing Composite Structure on NSRP Payloads.

By briefly discussing the benefits of using 6061-T6 is to suggest that a single composite material be identified as an alternate to 6061-T6. This composite material should be commercially available in common stock forms and pursuant to the design objective, have a lower density than 6061-T6. The stock forms identified in the NIACS are thin plates, prismatic elements, and hollow cylinders. Further, to maintain current program analysis practices, the selected composite material should be quasi-isotropic and homogeneous. This is to enable short payload design lifecycles, to limit the amount of structural analysis required on a per payload basis, and to continue to provide robust part designs that allow reciprocal use on other missions. To maintain electrical grounding and thermal practices, the composite material should be electrically and thermally conductive. It is also desired for the composite material to have published material properties.

Advanced engineered composite materials encompass several subcategories including polymer matrix composites (PMCs), metal matrix composites (MMCs), and ceramic matrix composites (CMCs). MMCs and CMCs are impractical for broad use on the NSRP as material costs far exceed those of similar monolithic materials. Further, the density of MMCs and CMCs are similar to 6061-T6 aluminum and offer no obvious benefit in terms of reducing payload mass. Considering PMCs, these materials are generally less dense than metals and, depending on their composition, meet or exceed material properties of the same. For this reason, there is potential to reduce payload mass using PMCs. Further, the cost of PMCs, while more expensive than most metals per unit mass, is less expensive than either MMCs or CMCs. PMCs will be the focus material subcategory for the NIACS reconfiguration.

PMCs are the most popular category of composite materials, encompassing a variety of fiber and matrix types. Common fiber materials include glass, carbon, and aramids. Common matrix materials include epoxy, phenolics, acrylic, urethane, and polyamides [8]. Recalling requirement four, only those composite materials that are ASTM E595 compliant will be allowed. Considering the need for the selected composite material class to be electrically conductive, and considering PMC matrix materials are insulative, the fiber material must be conductive. By process of elimination, a CFRP (Carbon Fiber Reinforced Polymer) best aligns with the reconfiguration requirements, programmatic needs, and norms for an alternative, default material to 6061-T6 aluminum.

This investigation will use two, specific, commercially available CFRPs for NIACS structural reconfiguration. The selection of these particular CFRPs does not constitute an endorsement or recommendation. The first material is CYTEC Carbon Fiber Prepreg 934 3K/PWC T300 UT. This commercially available, pre-impregnated fabric lamina has been widely used in aerospace applications for decades and is suitable for primary structures [9]. The fiber is Toray's T300, a three-thousand count filament. In this application, the T300 is arranged in a 2/2/1 plain weave fabric and impregnated with CYCOM® 934 epoxy resin. This prepreg is suitable for critical space applications and has a service temperature of 350°F. Not only is this material suitable for internal payload elements but also for external features, depending on payload location. This prepreg is autoclave cured. Considering payload part geometry, this material is well suited for plate elements such as the Regulator Bracket (Figure 32) and the Electronics Deck (Figure 8). The second material is intended for prismatic parts such as the

Pneumatic Umbilical Bracket (Figure 36) and Main Manifold Mounting Block (Figure 42). In their existing form, constructing these parts from a stacked sequence of prepreg is uneconomical. Instead, a compression molding technique using a BMC (Bulk Molding Compound) is suggested. The second material is Toray's MS-1A, a BMC with a service temperature of 350°F and density 44% lower than 6061-T6. Both T300 3K/934 and MS-1A are ASTM E595 compliant. Material properties for T300 3K/934 are provided in the *Composites Materials Handbook* (CMH-17) [9] while MS-1A material properties are provided by Toray data sheets [10].

After deconstructing the NIACS into its individual components, examining the current applications of 6061-T6 aluminum in the program, and identifying two viable composite materials as potential replacements, we now proceed with the reconfiguration process starting with the primary structure – the skin. The sounding rocket payload skin is the primary structure onto which internal substructures and external functional elements are attached. A majority of skins used on sounding rocket payloads are manufactured from a single forging of 6061-T6 aluminum. At 16.50 lb_m, the NIACS skin accounts for 20.2% of the total mass of the subsystem. If one were to substitute the NIACS skin material for CFRP, the mass of the skin would decrease by 7.07 lb_m, or 43%.

This seemingly obvious material substitution is complicated by skin joint geometry. Joints are necessary as they are the common interface that is foundational for the modular nature of NASA sounding rocket payload system design and allow personnel access to internal subsystems during integration, testing, and pre-flight operations. Joints are functionally necessary for in-flight payload separation from spent motor casings and ejection of adjacent skins to expose instruments to the space environment. One drawback to skin joints is a decrease in payload bending stiffness. Payloads with too many or poorly positioned joints, or joints with excessive slop and compliance, will deflect under aerodynamic loading, causing a decrease in the flexible stability margin of the sounding rocket under powered flight. Often the recourse for negative flexible stability margins is to increase the skin thickness, which increase payload mass, therefore affecting apogee and time above altitude metrics. Recalling the first design requirement, joint geometry must be maintained for the purpose of modularity. The NIACS skin has a forward male radax joint and an aft female radax joint. A simplified geometry of the radax joint is shown in Figure 44.

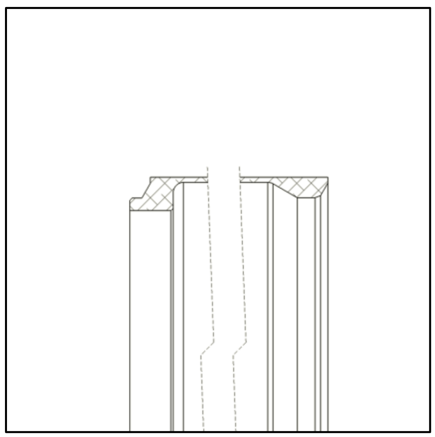

Figure 44: Radax Joint

This skin geometry is currently formed by removing material from a stock forging of 6061-T6 aluminum tube. To economically manufacture a single-piece NIACS skin from a CFRP, an additive process, such as fiber winding, would be required. To consider fiber winding further, a single-piece, conventional mandrel was designed onto which the NIACS skin could be wound, shown in Figure 45. In the figure, the checkerboard pattern represents the mandrel, and the fuchsia represents the spindle on which the mandrel rotates. In Figure 46, the fiber-wound skin part is shown in grey. In this setup, some waste material is generated, shown in red.

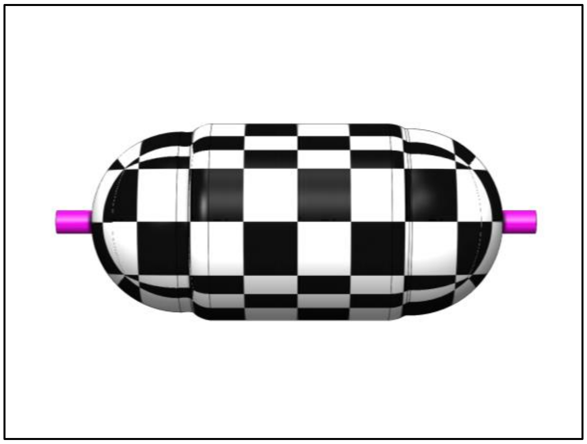

Figure 45: Filament Winding Mandrel

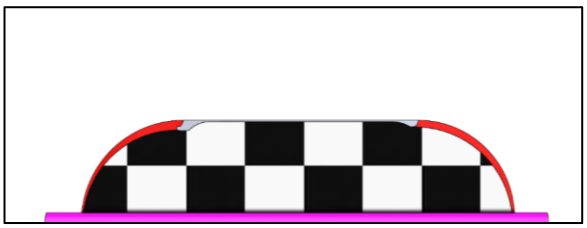

Figure 46: Filament Winding Mandrel Cross-Section

While it is conceivable to manufacture a single-piece, NIACS skin using the fiber winding process, it is impractical for broad use in NASA's sounding rocket program because skins have varying length and joint requirements. In practice, every skin (of which there are countless variations) needs a matched mandrel. The mandrel would need to have a dissolvable core in order to remove the skin from the mandrel intact or be a two-piece mold or clamshell tool. In addition to the initial forming of the skin on the mandrel, the skin will require detailed machining of joint geometry, including through-holes and tapped features for fasteners. CFRPs are not recommended as a base material for cut or formed threads so threaded inserts, nut plates, or another fastening system needs to be considered. Fastening methods alone necessitate joint redesign which is in violation of the first design requirement. Aside from the technical concerns, the initial assessment indicates this process is incompatible with the program due to its high cost.

An alternative approach to a single-piece, fiber wound skin is a hybrid, three-piece skin in which the joints are manufactured separately, then bonded to a CFRP cylinder, as shown in Figure 47. This approach maintains joint geometry, ensuring modularity, and simplifies the CRFP tube geometry to be purely cylindrical. The three parts are bonded into a single assembly using an epoxy such as LOCTITE EA 9394 AERO.

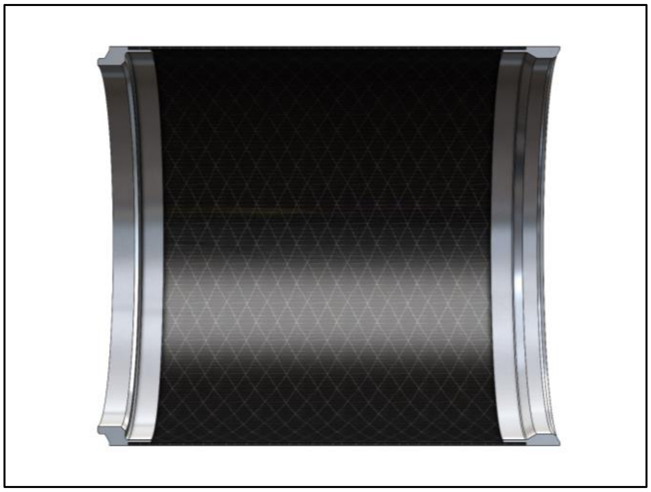

Figure 47: Three-Piece Composite Skin Cross Section

This approach is favorable to the single-piece CFRP skin as the tube length can change to meet mission specific needs while being procured in standard diameters and lengths. Further, joint details remain compatible with the current design approach and implementation, ensuring modularity. For comparison, using 6061-T6 joints, a NIACS, hybrid skin design has a mass of $14.09\ lb_m$, a reduction of $2.41\ lb_m$, or 17.1%. The mass reduction potential increases proportionally with skin length, as the bulk of the skin's mass is concentrated at the joints, as shown in Figure *48*.

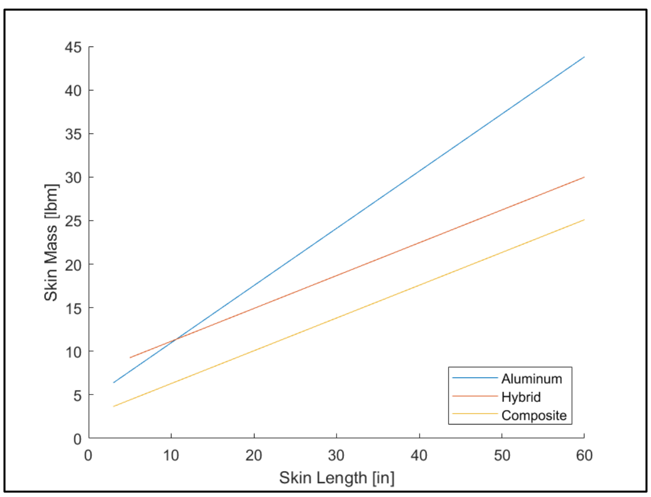

Figure 48: Skin Mass per Unit Length

There are limiting factors associated with the hybrid approach, such as galvanic corrosion between the joint rings and the tube. Galvanic current is high between carbon fiber and aluminum alloys. There are several mitigations such as using titanium instead of 6061-T6 for the joints or introducing an insulative material such as fiberglass between the galvanically dissimilar materials. Another limiting factor concerns payload recovery. NASA sounding rocket payloads are often recovered, refurbished, and re-flown. Due to low CFRP fracture toughness and plasticity, it is unlikely that a CFRP skin will be suitable for re-flight as significant internal damage can develop during low velocity impact [11]. Recycling flight hardware, especially skins, is a program principle and should be conserved in the hardware lifecycle. Many NASA sounding rocket skins are also hermetic. By introducing potential leak paths through the bonded joints, this may increase the sealed skin leak rates which risks mission success. Finally, and while not a hybrid approach specific issue, there are skin geometries that are not well suited to a constant diameter CFRP, specifically NASA sounding rocket telemetry skin assemblies which have recessed features for antennas.

By identifying these limiting factors and potential issues, it is evident that simply replacing aluminum skins with CFRP equivalents will be often incompatible with subsystem form, skin assembly function, and programmatic intent. It is reasonable that CFRP skins could be used on a case-by-case basis. However, the detailed design and lifecycle considerations of such a CFRP skin is beyond the scope of this investigation. Consequently, to maintain a conservative approach in the NIACS reconfiguration process, the skin will remain as designed.

The following sections examines the internal substructures, skin assembly, and components. Sounding rocket subsystem secondary structures are typically flat plates (decks or bulkheads), rigidly mounted to the skins by either radial attachment or to longitudinally oriented flanges, located along the payload body. Most internal structures, if not a single deck, are cantilevered from longeron structures. The NIACS internal substructure is composed of two assemblies, an avionics assembly, and a pneumatic assembly. By having two standalone subassemblies, each is able to be built and tested separately from the other. As seen in Figure 49, the avionics assembly is supported by a thick, aluminum deck with cavities on the aft face to recess four batteries, hence decreasing the overall length and mass of the NIACS system. The deck thickness is about one inch and has a mass of 6.85 lb_m.

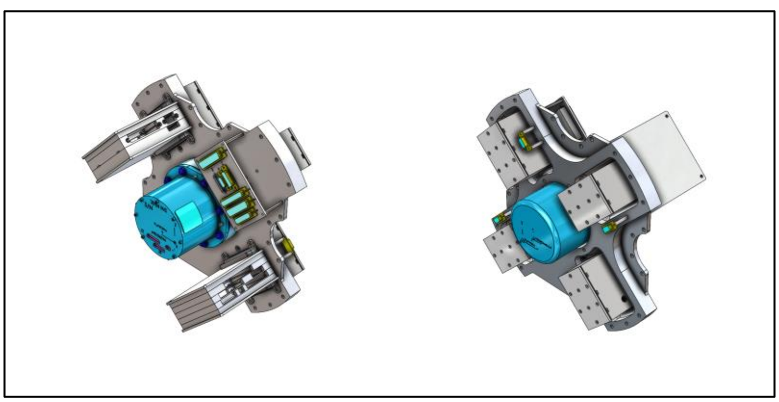

Figure 49: Avionics Assembly

The TERN IMU is mounted to a Lift Ring, an adapter to the bolt pattern for the legacy IMU, the GLNMAC. The two electronics board stacks are for the avionics and power system. Four D-subminiature connectors on the aft surface of the assembly are for the batteries while the D-subminiature connectors on the forward surface are for avionic interconnects. All connectors are supported with standoffs.

The pneumatics assembly (Figure 50) provides structure for two pneumatic tanks and various manifolds, regulators, valves, fittings, and tubes. The primary element onto which the tanks are mounted is the Tank Cradle (Figure 19). Each tank is strapped to two of the Tanks Cradles using a pair of Tank Restraint Clamps, padded with Tank Cushions.

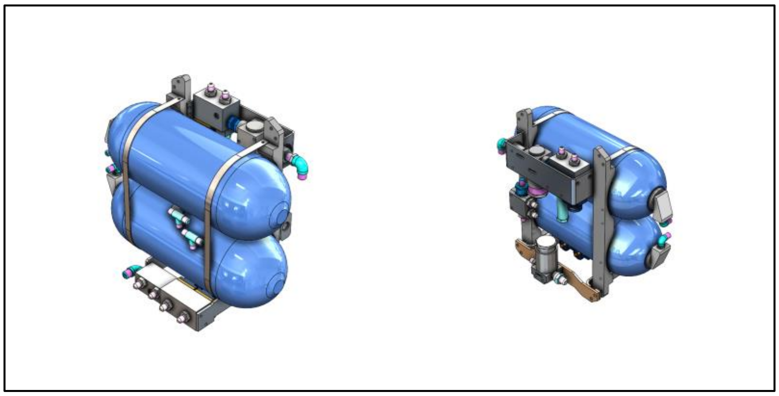

Figure 50: Pneumatics Assembly

The other parts of this assembly are sheet metal, formed to mount the manifolds and regulators off the Tank Cradle. All pneumatic tubing is simply supported, that is, only rigidly connected at its ends. The pneumatic components are positioned around and below the tanks, strategically located in case of replacement. As discussed earlier, the joints in the skin are necessary for personnel access. In this case, if a valve or regulator were to need to be replaced, the aft radax joint could be disassembled to allow personnel access to the internal assembly.

The NIACS skin assembly and skin-mounted hardware are shown in Figure 51. There are two sets of four, deck mounting brackets that support the NIACS avionics subassembly and the NIACS pneumatic subassembly. There are also two roll control blocks, and four transverse nozzle blocks. A doubler is riveted to the skin which provides backing and mounting for a recessed door. The door provides access to the internal assemblies if components need to be replaced and to decompress the pneumatic system after flight and before handling.

Figure 51: NIACS Skin Assembly

The initial structural reconfiguration approach for the two subassemblies was first to simply change part material from 6061-T6 to a CFRP, either the T300 3K/934 or MS-1A depending on the form of the part. This approach, though simple, fails to capitalize on material property improvements and fabrication methods possible with these materials. For example, fabricating the *Electronics Deck* from a CFRP in its original form would be wasteful in terms of production cost as the deck is near one inch thick. A comparable deck fabricated from T300 3K/934 composite would conservatively require only half the thickness of its aluminum counterpart. Similarly, many of the sheet elements in the pneumatics assembly could be merged into a single part, decreasing the number of unique parts and fasteners. Thus, a revised strategy of reconfiguring the NIACS internal assemblies to leverage the unique material properties and manufacturing methods possible with CFRPs is suggested. Two options are considered. The first is to keep the generic form of the two subassemblies, that is, deck-based structures for the avionics subassembly and a cradle-based structure for the pneumatics subassembly. The second option is to combine the two subassemblies into a single subassembly to further reduce the number of parts such as deck mounting brackets and their corresponding mounting details.

The second strategy was selected because a single subassembly would likely reduce the overall part count, thereby decreasing total mass compared to two separate subassemblies. This approach may also decrease manufacturing cost as, generally, part count and fabrication cost have an inverse relationship. This strategy may also simplify assembly operations. In its current architecture, the avionics subassembly is assembled, tested, then installed in the skin assembly through the forward radax joint. Meanwhile, the pneumatics subassembly is assembled in the skin itself as the rigidity of its substructure is dependent on the skin. Assembling the pneumatics subassembly in the skin is problematic for two reasons. The first is skin assembly availability. Skin fabrication requires approximately forty-two machine hours spread over several months which may cause delays in system integration if not completed on schedule. Personnel access is another key consideration, as assembling the system within an enclosed volume presents greater challenges than working in an open configuration. The downside to this single substructure approach is the inability to build and test the avionics and pneumatics assemblies separately. Considering the existing design of the NIACS, how it is assembled and tested, the following single-piece substructure is proposed (Figure 52).

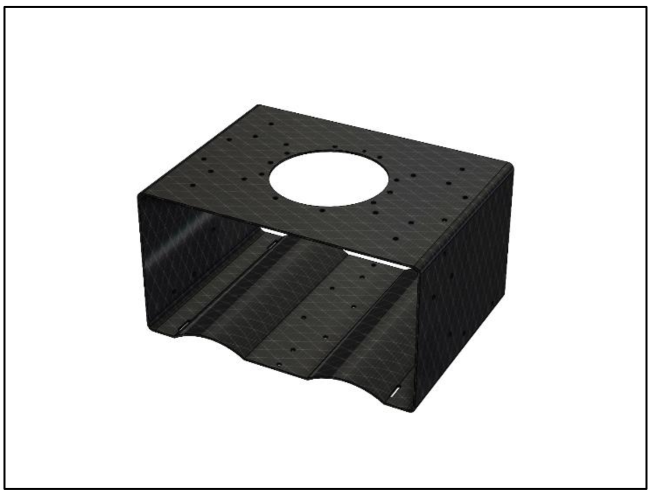

Figure 52: Proposed NIACS Substructure

This substructure has basic dimensions of $8.00\ in\ x\ 10.75\ in\ x\ 5.75\ in$. The thickness of the substructure will be refined but was initially estimated to be $0.08\ inches$, or ten layers of the T300 3K/934 prepreg lamina. The form is a four-sided, hollow, rectangular prism with a circular cutout on the top surface for the TERN IMU and cylindrical concave features on the bottom surface for two gas tanks. Initial part weight is $1.09\ lbs$. Figure 53 shows the beginning of the internal assembly with the IMU and gas tanks in position.

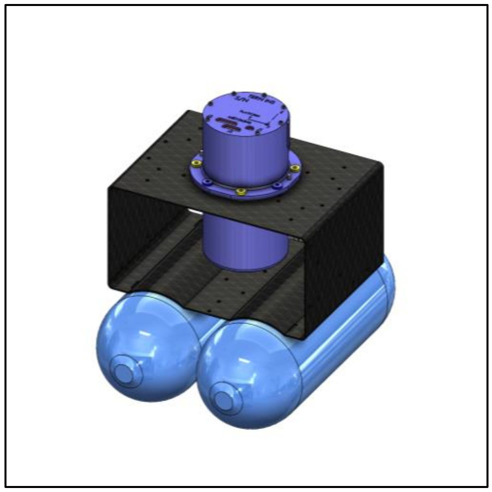

Figure 53: Major Components Mounted on Substructure

One strategy to decrease the mass of the NIACS is to decrease the overall length of the system. The primary factor that determines the length of the system is the height of internal assemblies. Comparing the existing substructure layout (left) to the updated layout (right) in Figure 54, one observes how the components in the reconfigured design have been positioned closer to one another to decrease system length.

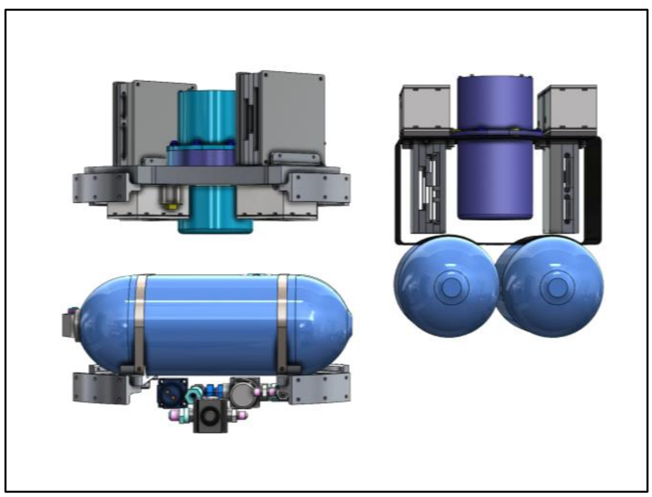

Figure 54: Internal Substructure Comparison

The design of the substructure is such that it is self-supporting and allows for components to be mounted to eight unique surfaces as opposed to two surfaces for a single deck. This approach makes better use of the internal volume of the skin and decreases the number of internal substructures and supporting elements. Figure 55 shows the batteries, power distribution system, and flight computer in position on the substructure. The batteries are positioned on the top surface for several reasons. The first being that the height of the batteries is shorter than the top surface of the TERN, limiting the height of the internal assembly. The second reason is for accessibility, both for connecting and disconnecting the power source from the power distribution system and for replacing batteries during testing and launch operations.

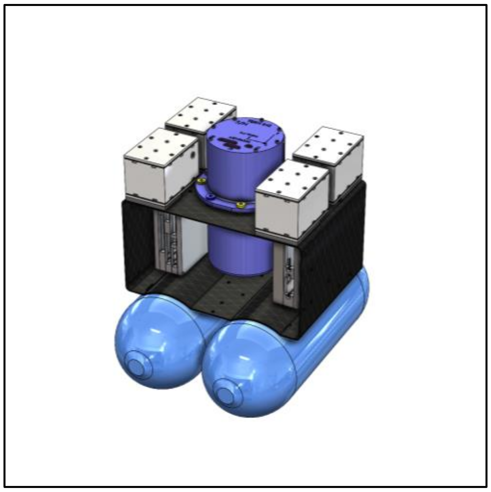

Figure 55: Power System and Avionics Mounted on Substructure

Next, the pneumatic components are added to the assembly. This NIACS configuration is what is known as a bi-level system, that is, there are two pressure modes the system can operate under depending on the maneuver type and desired pointing accuracy. The “coarse” level is for large maneuvers such as slewing the payload from an Earth zenith attitude to a negative magnetic field attitude. A maneuver such as this must be done in a short amount of time (on the order of seconds) to take advantage of the upleg trajectory observation period. This mode is also known as the high-pressure mode. The second mode is a “fine” level which provides higher pointing accuracy and less jitter than the “coarse” mode. This mode is also known as the low-pressure mode.

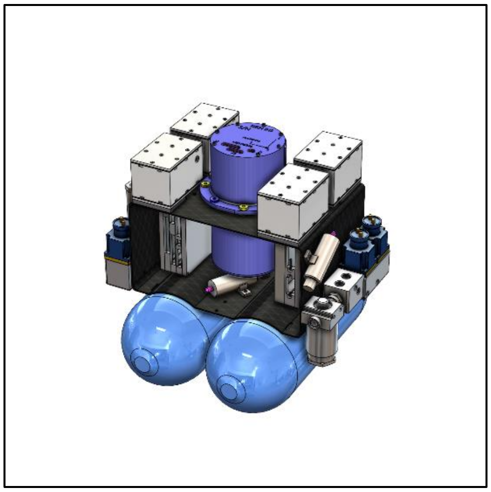

Figure 56: Functional Components Mounted on Substructure, Isometric

The redesigned NIACS positions the high-pressure manifold and bi-level transfer valve on one side of the assembly and the main manifold on the other. This arrangement provides physical separation between the high-pressure regulator and low-pressure regulator, limiting human factor error when the regulator pressure is set. The position and orientation of the manifolds, check valves, relief valves, and pressure transducers were dependent on the available space in the assembly but conform to the original pneumatic configuration, as detailed in a separate schematic (not provided). Component placement was considered in order to facilitate connection via rigid tubing. Side-views of the assembly without rigid tubing are shown in

Figure 57.

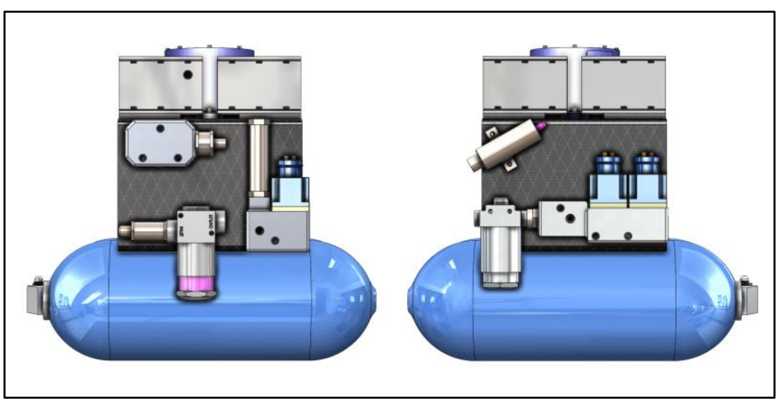

Figure 57: Functional Components Mounted on Substructure, Side Profiles

Next, all rigid tubing and pneumatic fittings are added to the assembly, seen in Figure 58. Pneumatic tube size matches that of the existing NIACS configuration. In the subassembly, there are ten tubes; each has been formed such that the minimum bending radius has not been exceeded.

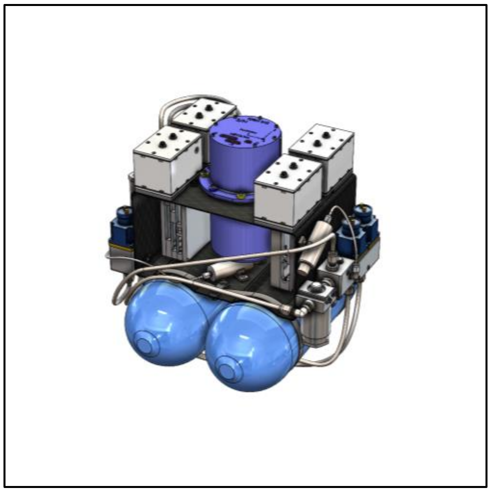

Figure 58: NIACS Subassembly, Isometric

Throughout the design process, consideration was given to how each component will attache to the CFRP substructure. The most common fastening scheme used on NASA sounding rocket payloads are threaded fasteners into tapped thru holes in the base material. While drilling and tapping or forming threads into a CFRP is possible, it is not a recommended method [12]. Given this, an alternative approach, using adhered nut plates, is employed. Nut plates are a common approach in the aerospace industry when threaded features are required. For this application, the selected nut plate is a Click Bond® CN609. The nut plate is adhered to the composite substrate using a proprietary adhesive. To decrease the number of unique parts in the assembly, all fasteners are #8-32 NAS SHCS (Socket Head Cap Screws). This conformity allows for a single nut plate part number to be used. One downside to this approach is that it is difficult to mount components on opposing sides of the structure as the nut plate is where another component would otherwise be located. This was problematic for mounting the batteries, avionics, and power system on opposing sides of the topmost surface. To avoid part interference and to allow efficient packaging of the internal assembly, adapter plates for the batteries, avionics, and power system were designed (see Figure 59). The proposed material for these nonstructural parts is MS-1A.

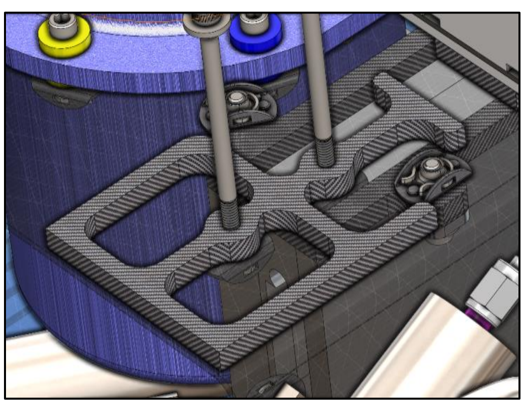

Figure 59: Battery Standoff Plate

One additional part needs to be considered for the internal subassembly, that is a means to attach the substructure to the skin. Being that the substructure in the new assembly has changed drastically, a new part must be designed. The general approach for mounting substructures inside payload skins is to provide mounting from the aft most position, to avoid suspending assemblies from bulkheads or decks by fasteners alone, and to use radial skin attachment methods, via deck brackets, as shown in Figure 51. With this understanding, an integrated substructure support is proposed, shown in Figure *60*, the Integrated Substructure Support.

The substructure support mimics the electronics deck design (Figure 61). The substructure support mounts to the skin assembly in a similar method as the original NIACS, via deck mounting brackets. The substructure support, like the substructure, has concave features to conform to the gas tanks. To attach the substructure support to the substructure, two stainless steel straps are routed through cutouts on each part. When the straps are tightened, the compression couples the structure and substructure support to the gas tanks. Strap compression is the current method used to attach the gas tanks to the NIACS pneumatic assembly (Figure 50). The proposed material for the substructure support is T300 3K/934 as it resembles a flat plate.

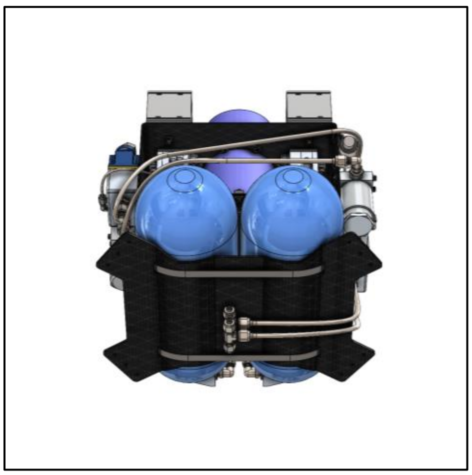

Figure 60: Integrated Substructure Support

Figure 61: Electronics Deck and Substructure Support Comparison

With critical components integrated into the substructure, the focus shifts to the skin assembly. The skin retains all functional features including the forward and aft radax joints, lanyard, and umbilical details, and a single door at the 180° position. While additional doors at the 90º and 270° position would be beneficial for personnel access, they are omitted for the sake of parity between the original and reconfigured NIACS. The current design practice is to have inset doors that are diametrically coincident with the outside surface of the skin to reduce drag on exposed faces and edges. This design strategy requires a doubler be installed on the inside diameter of the skin to provide backing and sufficient thread engagement for the door fasteners. The doubler is typically riveted to the skin and will remain 6061-T6 for the sake of retaining threaded through holes. However, the door material will be changed to MS-1A (Figure 62). Like other parts using BMC, the manufacturing method for this door will be compression molding which lends itself well to forming integrated ribs on the inside diameter of the door. This allows the door panel thickness to be reduced while retaining sufficient strength to resist dynamic pressure on the payload body.

Figure 62: Skin Assembly Door and Doubler

Revisiting Figure 54, the skin length can be decreased because the height of the internal subassembly has decreased. The original skin length was 19.5 inches. With the enhancements made to the internal subassembly, the reconfigured NIACS skin length decreases to 16.5 inches. This 3 inch reduction is significant in terms of overall subsystem mass and will decrease aerodynamic drag and moments of inertia of the payload, especially the payload pitch moment of inertia about the payload center of mass.

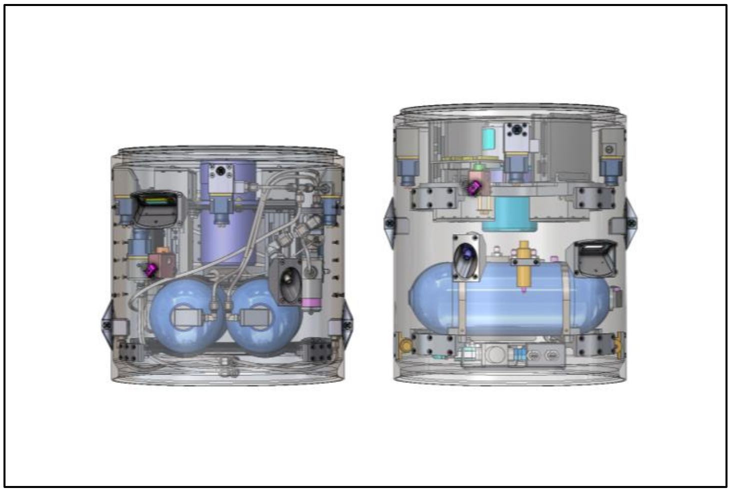

Figure 63: Skin Length Comparison

The pneumatic components within the skin assembly*,* including the transverse nozzle blocks and roll control block*s*, remain 6061-T6 as stated in the requirements. The position of the transverse nozzle blocks remains on the forward side of the skin assembly while the roll control blocks have been moved aft to eliminate interferences in the new assembly. Their position has no bearing on function. Pneumatic tubes and fittings also retain their existing materials.

Figure 64: NIACS Skin Mounted Components

Select skin mounted components have been considered for a material change from 6061-T6 to a CFRP. One such part is the universal umbilical bracket. This bracket is one of a two-part assembly whose function is to provide mounting for a 50-pin D-Subminiature connector which interfaces with the NIACS GSE (Ground Support Equipment). The universal umbilical bracket is shown in Figure 33. Of all the parts in the NIACS assembly, the universal umbilical bracket is most prevalent in NASA sounding rocket payload subsystems. Most payloads have multiple of these brackets as it can accommodate many types of connectors (D-Subminiature, BNC, Fiber Optic SC, etc.) depending on subsystem requirements. This part is currently manufactured from a single block of 6061-T6 aluminum stock. To decrease the mass of the bracket, using MS-1A is proposed, reducing the mass of the bracket by $0.20\ lb_m$, or 25%. Similarly, the pneumatic umbilical bracket (Figure 36) and deck mounting bracket (Figure 35) are well suited to be manufactured from MS-1A and would also see reduced part mass of 25%. As all these parts are formed from a BMC via a compression molding process, molds will need to be designed, and the parts modified to have sufficient drafts and ejection points from the mold. These features and the compression molding process will be briefly discussed during the cost analysis.

This concludes the initial structural reconfiguration of the NIACS subsystem. This assessment has been performed to determine if subsystem parts can be fabricated using composite materials. For those structural parts identified to be fabricated from composite materials, failure analysis must be conducted to determine critical dimensions and part characteristics that will influence the mass and cost of each part. Nine unique parts were identified during initial configuration design to be manufactured from CFRPs. Of these, three are structural - the substructure, substructure support, and deck mounting bracket. The remaining CFRP parts serve non-structural functions and thus do not require failure analysis. Following failure analysis, a Bill of Materials for the reconfigured NIACS will be presented, detailing the final mass of each component.

Analysis of the structural CFRP elements will be conducted as a preliminary design-analysis. The goal is to demonstrate that the CFRP structural elements of the reconfigured NIACS assembly will withstand the loading environment of a NASA sounding rocket payload. In practice, iterative failure analysis would be used to minimize part mass via optimization. However, this is beyond the means of this investigation as minute differences in reconfigured NIACS mass will not be evident in the carpet plots used to estimate performance metrics. As all CFRP parts are internal to the payload, thermal effects will not be considered.

A core philosophy of the NASA Sounding Rocket Program is to test payload hardware in excess of the flight environment. As each NASA sounding rocket mission is unique, constituting different launch vehicles, payload characteristics, and launch conditions, a random vibration testing profile has been established which encompasses all flight environment factors and variability. This random vibration profile is described in the NASA Sounding Rockets User Handbook, Table 6.3.4-1 (Vibration Test Levels for new Payload Designs), shown below in Table 5 [1].

	Vehicle Level One	Vehicle Level Two
SINE	Sweep Rate: 4 oct./min. Test Profile: 3.0 in./s 10-144 Hz 7.0 g 144-2000Hz **THRUST AXIS ONLY**	Sweep Rate: 4 oct./min. Test Profile: 3.84 in./s 5-24 Hz 1.53 g 24-110 Hz 3.50 g 110-800 Hz 10.0 g 800-2000 Hz **THRUST AXIS ONLY**
RANDOM	Duration: 20 sec./axis Thrust Axis Spectrum: 10.0 grms 0.051 g^2/Hz 20-2000 Hz Lateral Axis Spectrum: 7.60 grms 0.029 g^2/Hz 20-2000 Hz	Duration: 10 sec./axis Spectrum: 12.7 grms 0.01 g^2/Hz 20 Hz 0.10 g^2/Hz 1000 Hz (on 1.8 db/oct. slope) 0.10 g^2/Hz 1000-2000 Hz **SAME IN ALL AXES**
TEST INFO	**LEVEL 1 VEHICLES** Single Stage Improved Orion Terrier MK12 – Improved Orion Terrier MK12 – Malemute Terrier MK12 – Lynx	**LEVEL 2 VEHICLES** Single Stage Black Brant Terrier MK12 – Improved Malamute Terrier MK70 – Improved Orion Terrier MK70 – Malamute Terrier MK70 – Improved Malamute Terrier MK70 – Lynx Terrier MK70 – Oriole Black Brant IX Black Brant X Black Brant XI and XIa Black Brant XII and XIIa

Table 5: Vibration Test Levels for New Payload Designs

Preliminary design-analysis is based on NASA-STD-5002A (Load Analyses of Spacecraft and Payloads). For preliminary, random vibration load factors, the standard suggests utilizing "three times the composite GRMS of the specified random vibration environment" [13]. This recommendation stems from the fact that random vibration limit, quasi-static loads typically represent the three-sigma load case. Thus, the NIACS external load factor will be:

$$G \equiv 3 \times G_{RMS} = 3 \times 12.7\ G_{RMS} = 38.1\ G \tag{4}$$

As this is a preliminary design-analysis, not all parts are in their as-built form. Also, hardware and electrical components are absent from the assembly at this phase. Thus, mass estimates of their contribution to the three composite structural parts will be estimated to be 45 lb_m. While the random vibration, quasi-static load factor can be applied in any direction, for simplicity, a single load case will be analyzed. This load case will be coaxial with the payload principal axis, oriented aft. The line of action is colinear with the theoretical rocket motor thrust. In practice, this load case is one of the three vibration test directions. In flight, loads may be directed from any direction. Free-body diagrams of the three structural CFRP parts are shown in Figure 65 through Figure 67.

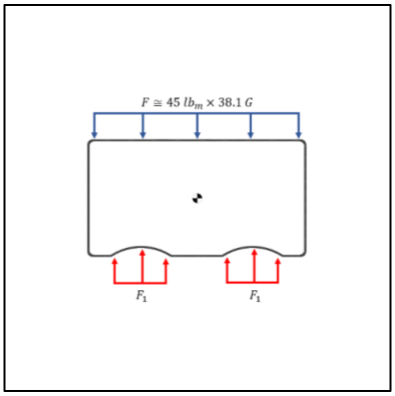

Figure 65: Substructure Free Body Diagram

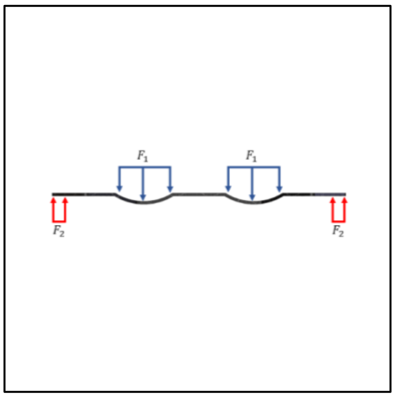

Figure 66: Substructure Support Free Body Diagram

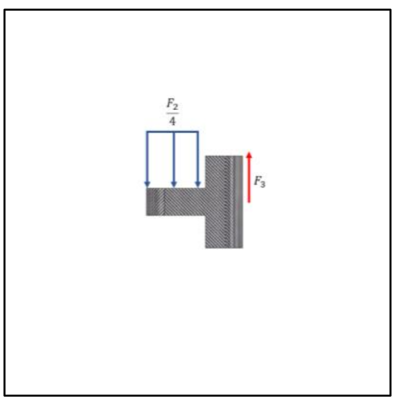

Figure 67: Deck Bracket Free Body Diagram

The means of the preliminary design-analysis will be finite element analysis (FEA) using SolidWorks Simulation Premium. Material properties for T300 3K/934 are taken from CMH-17 Volume 2 [9]; material properties for MS-1A are taken from Toray data sheets [10]. The T300 3K/934 model type is linear elastic orthotropic while MS-1A is linear elastic isotropic, due to the random orientation of fibers within the BMC. For parts proposed to be made from T300 3K/934, the part is represented as shells then each shell is characterized as a composite element. In keeping with the prescribed layup strategy discussed earlier, each plies orientation is the same (notionally zero degrees), so the composite stacking sequence is inherently symmetric.

Mesh parameters are consistent for parts made from T300 3K/934. Mesh elements are curvature-based with a growth rate of 1.2 and minimum element size half the ply thickness. The maximum element size is two orders of magnitude larger than the minimum element size. For the deck bracket, the minimum element size is half the smallest fillet radii. The maximum element size is again, two orders of magnitude larger than the minimum element size. The mesh Jacobian ratio was confirmed to be less than ten for each part, with most elements' ratios being one. Finite element analysis was conducted within an assembly to reduce fixture inaccuracies. Component interactions were global, and each model was stabilized using the soft springs method.

The substructure is estimated to support 45 lb_m of components, hardware, and wiring. The force resulting from the quasi-static acceleration of the random vibration environment is subjected to the top surface of the substructure (Figure 68). Anecdotally, this is a conservative case for the preliminary design-analysis.

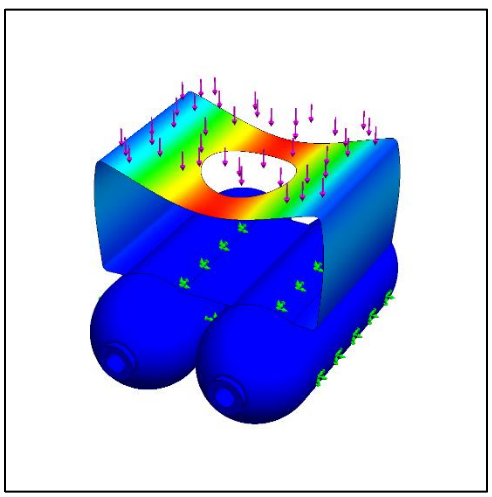

Figure 68: Substructure FEA FOS Color Map

The goal of the analysis is to demonstrate the CFRP structural elements of the reconfigured NIACS assembly will withstand the loading environment of a NASA sounding rocket payload. This equates to factors of safety greater than one for all elements in and across all layers of the composite material in the FEA. In this preliminary design-analysis, the independent variable is the number of layers of lamina composing the substructure. The process is to iteratively change the number of layers, evaluate the minimum factor of safety across all plies of the part, then increase or decrease the layers until the resultant factor of safety is greater than one. For the substructure, the initial guess was twenty plies of T300 3K/934. The resultant, minimum factor of safety was recorded for all iterations and was found to converge (Figure 69). The minimum number of plies for the substructure in this load condition was found to be twenty-eight, with a part minimum factor of safety of 1.05.

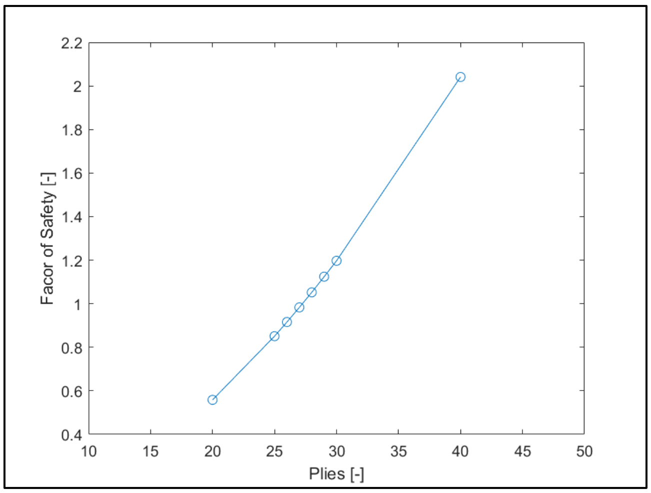

Figure 69: Substructure FEA Factor of Safety per Plies

A similar process and initial conditions are used for the substructure support. The minimum number of plies was found to be forty-four with a minimum factor of safety of 1.01. See Figure 70 for a graphic showing fixtures, loads, and the factor of safety color map of the substructure support. Like the substructure, the minimum factor of safety across all plies converged, see Figure *71*.

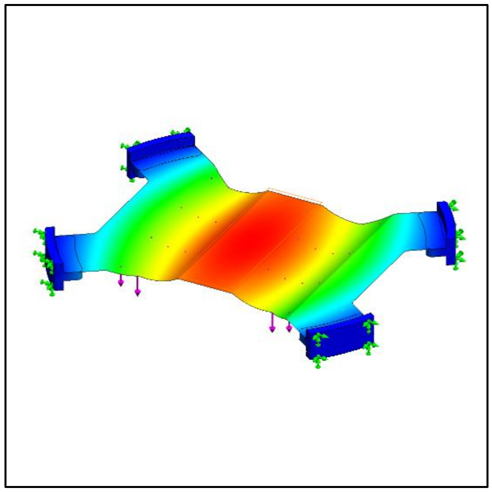

Figure 70: Substructure Support FEA FOS Color Map

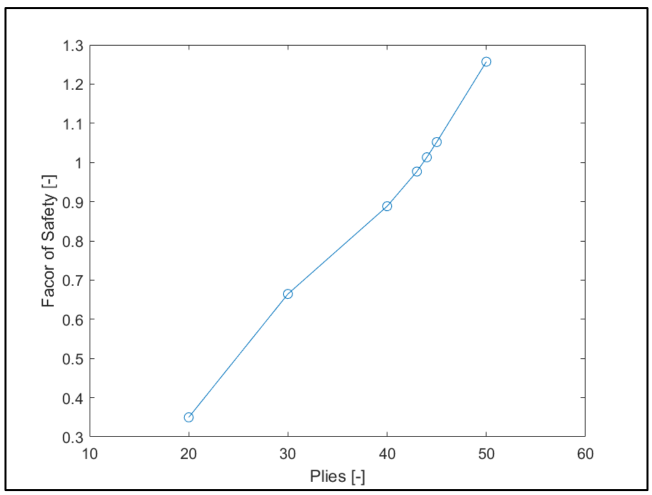

Figure 71: Substructure FEA Factor of Safety per Plies

The process for the deck mounting bracket was different than the substructure and substructure support as part composition is not based on plies of lamina. The intent of the analysis was not to optimize part geometry but rather to determine whether the proposed geometry would withstand the quasistatic acceleration loading of the internal assembly. Assuming the skin is perfectly ridged, the outside diameter elements of the deck mounting bracket were assigned fixed geometry while the support surface was subjected to the quasistatic load. Overall, the deck mounting bracket minimum factor of safety was 1.05. No geometry change is necessary at this phase.

For the purpose of this investigation, only structural, CFRP based parts have been analyzed by means of preliminary design-analysis. Each part has been shown to withstand the loading environment of a NASA sounding rocket payload and for substructure and substructure support, the number plies has been established. In practice, each part will require additional analysis and may be optimized for mass. Having finalized structural part geometry for this phase of the design, the next step is to determine the reconfigured NIACS mass. The Bill of Materials for the reconfigured, composites-based, NIACS is given in Table 6.

Item Number	Description	New Part	Modified Part	Quantity	Material	Mass (lb_m)	Mass Delta (lb_m)
1	NIACS Skin Assembly			1			
1.1	Skin		✓	1	6061-T6	14.44	-2.10
1.2	Skin Door		✓	1	MS-1A	0.29	-0.09
1.3	Skin Doubler		✓	1	6061-T6	0.35	-0.09
1.4	Umbilical Bracket Assembly			1			
1.4.1	Universal Umbilical Bracket		✓	1	MS-1A	0.20	-0.16
1.4.2	Umbilical Backing Plate			1	6061-T6	0.01	0.00
1.5	Deck Mounting Bracket		✓	4	MS-1aA	0.12	-0.25
1.6	Pneumatic Umbilical Bracket		✓	1	MS-1A	0.20	-0.16
1.7	Transverse Nozzle Block, Right		✓	2	6061-T6	0.52	-0.04
1.8	Transverse Nozzle Block, Left		✓	2	6061-T6	0.52	-0.04
1.9	Roll Control Block			2	6061-T6	0.57	0.00
2	NIACS Internal Subassembly			1			
2.1	Substructure	✓		1	T300 3K/934	3.00	N/A
2.2	Battery Standoff	✓		4	MS-1A	0.04	N/A
2.3	Power System Standoff	✓		1	MS-1A	0.05	N/A
2.4	Flight Computer Standoff	✓		1	MS-1A	0.05	N/A
2.5	Power System			1			
2.5.1	Frame Top		✓	1	6061-T6	0.21	0.01
2.5.2	GIPS Distribution Frame			1	6061-T6	0.16	0.00
2.5.3	GIPS Regulation Frame		✓	1	6061-T6	0.36	-0.12
2.6	Flight Computer			1			
2.6.1	Frame Top		✓	2	6061-T6	0.21	0.01
2.6.2	Driver Board Frame			1	6061-T6	0.10	0.00
2.6.3	GIPS Power Entry Frame			1	6061-T6	0.11	0.00
2.6.4	ACS Flight Processor Frame			1	6061-T6	0.91	0.00
2.7	Substructure Support	✓		1	T300 3K/934	2.28	N/A
2.8	Tank Manifold			2	6061-T6	0.15	0.00
2.9	Tank Restraint Clamp		✓	2	201 Stainless	0.12	0.04
2.10	High Pressure Manifold		✓	1	6061-T6	0.57	-0.27
2.11	Strap Guide	✓		2	MS-1A	0.01	N/A
2.12	Bi-Level Transfer Manifold			1	6061-T6	0.65	0.00
2.13	Main Manifold		✓	1	6061-T6	1.09	-0.02

Table 6: Composite-Based NIACS Bill of Materials

A total of forty-two NSROC manufactured parts are required for the composites-based NIACS. Of these, twenty-seven parts are unique, ten are manufactured from composite materials, and six are new parts, absent in the original NIACS. The original NIACS required sixty-three NSROC manufactured parts, of which, thirty-eight are unique. By integrative design and using composite materials, the part count of NSROC manufactured parts has decreased by twenty-one parts, a reduction of 33%.

The CAD model of the composites-based NIACS must be mass accurate to compare against the original NIACS which has measured, empirical mass properties. To this end, all pneumatic tubes, fittings, fasteners, and other hardware has been modeled in the composites-based NIACS CAD. Yet, the model is incomplete as electronic components and harnesses are absent. However, the mass of the electronic components was measured from an as-built avionics system. The mass contribution of the electronic components is $5.34\ lb_m$.

Using the Mass Properties tool in SolidWorks, the mass of the redesigned NIACS is estimated to be $62.79\ lb_m$. Adding the electronics mass, the mass of the assembly increases to $68.13\ lb_m$, a reduction of $13.37\ lb_m$, or 19.6% of the original NIACS mass.

TRAJECTORY ANALYSIS

The structural reconfiguration of the NIACS serves as a representative estimate for potential payload mass reduction. The NIACS is a standard subsystem, composed of parts that are similar in form to other NSROC subsystems and general payload architecture. Thus, the 19.6% mass reduction achieved by the composites-based NIACS is extrapolated to the payload assembly in entirety to estimate the launch configuration mass. This mass reduction is extended to all missions launched in fiscal year 2024, shown in Table 7.

Mission Number	Original Payload Mass (lb_m)	Estimated Composites-Based Payload Mass (lb_m)
36.386 UE	977.5	785.9
36.387 UE	961.4	773.0
36.388 UE	964.8	775.7
36.375 UG	1262.6	1015.1
45.007 GE	1065.6	856.7
52.009 AE	967.6	778.0
36.392 UE	677.3	544.5
36.393 UE	666.2	535.6
36.394 UE	673.2	541.3
36.370 US	1070.5	860.7
36.371 NS	1183.0	951.1
36.396 UG	1104.0	887.6
41.133 WO	665.4	535.0
36.385 NS	982.6	790.0
46.042 WO	874.0	702.7
36.384 UG	1209.6	972.5
36.366 US	1179.4	948.2

Table 7: Fiscal Year 2024 Composites-Based Payload Mass

Trajectory metrics, specifically the apogee and time above the Kármán Line, are estimated using carpet plots in the *Sounding Rocket Users Handbook* [1]. For each mission in Table 7, the metrics of interest were located on the carpet plot for both the original payload launch configuration and the composites-based payload launch configuration. The launch elevation angle for each mission is given in NSRP mission documents. To increase the precision of the results, graduated lines were added to the carpet plots. In most instances, this allowed a precision of one kilometer apogee and five seconds above the Kármán line. Comparing the carpet plot results to the TAOS generated trajectories for each mission showed that the carpet plots underestimated payload performance as compared to the TAOS generated trajectory. However, the difference between these two methods is presumed to be constant. Therefore, the delta values were added to the TAOS trajectory metrics to determine the composites-based payload launch configuration performance. Figure *72* shows the apogee ordinates for mission 36.386 UE on the carpet plot for a Black Brant IX (Mod 2) from WSMR. The results for all fiscal year 2024 missions are shown in Table 8.

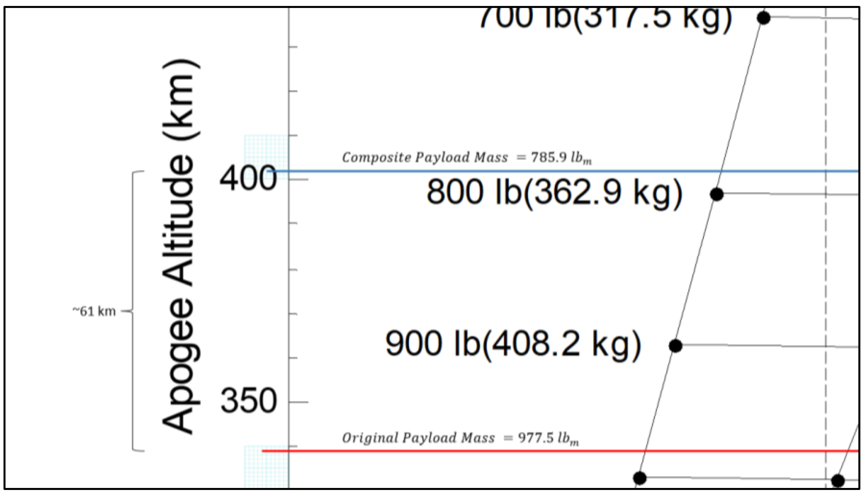

Figure 72: 36.386 UE Carpet Plot Apogee Delta

Mission Number	Original Apogee (km)	Delta Apogee (km)	Composite Payload Apogee (km)	Apogee % Delta	Original Time Above Kármán Line (s)	Delta Time Above Kármán Line (s)	Composites Payload Time Above Kármán Line (s)	Time Above Kármán Line % Delta
36.386 UE	341.3	61	402.0	17.8%	469.0	60	529.0	12.8%
36.387 UE	346.0	66	412.0	19.1%	473.4	65	538.4	13.7%
36.388 UE	344.8	66	410.8	19.1%	472.3	65	537.3	13.8%
36.375 UG	261.3	58	319.3	22.2%	376.7	64	440.7	17.0%
45.007 GE	322.3	63	385.3	19.5%	448.8	68	516.8	15.2%
52.009 AE	472.0	112	584.0	23.7%	602.1	90	692.1	14.9%
36.392 UE	407.6	68	475.6	16.7%	533.3	61	594.3	11.4%
36.393 UE	412.6	63	475.6	15.3%	537.6	57	594.6	10.6%
36.394 UE	409.5	60	469.5	14.7%	534.9	54	588.9	10.1%
36.370 US	262.8	59	321.8	22.5%	378.7	63	441.7	16.6%
36.371 NS	261.1	57	318.1	21.8%	375.9	65	440.9	17.3%
36.396 UG	285.6	42	327.6	14.7%	427.8	43	470.8	10.1%
41.133 WO	119.5	22	141.5	18.4%	128.7	64	192.7	49.7%
36.385 NS	338.8	62	400.8	18.3%	449.2	59	508.2	13.1%
46.042 WO	162.3	37	199.3	22.8%	231.4	64	295.4	27.7%
36.384 UG	272.4	60	332.4	22.0%	396.4	64	460.4	16.1%
36.366 US	276.5	60	336.5	21.7%	394.5	64	458.5	16.2%

Table 8: Trajectory Metrics

COST ANALYSIS

Changing the material and fabrication method of sounding rocket payload parts from conventionally machined aluminum to additively formed CFRPs may change the production cost of the system. As the NSRP is conducted under the H-LCAS program element, direct mission costs may impact the quantity of missions launched on an annual basis. Manufacturing costs for composite-based systems may outweigh their performance benefits, conflicting with program objectives. The adoption of composite parts may be hindered on the program if their production timelines exceed the established production lifecycle. To address these concerns, a cost analysis is performed.

The scope of the cost analysis will be those parts that are manufactured by the NSROC and COTS parts that are not present in the original NIACS. While fasteners, pneumatic tubes, and fittings are presumed identical in both systems, the composites-based NIACS incorporates adhered nut plates that are absent in the original design. These nut plates should be factored into the cost analysis of the composites-based system.

The cost of manufactured parts and unique COTS components will be assessed on a per system basis. The cost model is based on the detailed methods approach as the form of each part in both the original NIACS and the composites-based NIACS are established, despite the composites-based NIACS being in the intermediate-design phase. The cost of each system is the sum of costs for each part in the parent assembly. The cost per piece is determined by Equation (7) where C_{pc} is the *Cost per Piece*, C_m is the *Starting Material Cost*, C_L is the *Labor Cost Rate*, and T_p is the *Average Production Time Per Piece* [14].

$$C_{pc} = C_m + (C_L)T_p \tag{7}$$

Two omissions from Equation (7) are the *Equipment Cost Rate* and *Cost of Tooling*. The objective is not to provide a true cost of each system but rather to provide a relative difference in cost based on material and labor costs alone. Thus, it is assumed that the *Equipment Cost Rate* and *Cost of Tooling* are negligible. In this context, the *Cost of Tooling* includes machine tools needed for conventional machining as well consumables for composite material production such as vacuum bags and release films. Thus, the system cost is defined by Equation 8.

$$C_{NIACS} = \sum_{i=1}^{Part\ Count} C_{p_i} + \sum_{j=1}^{COTS\ Count} COTS \tag{8}$$

The labor cost rate is assumed to be the same for all parts, whether produced by material removal processes or by additive processes. Labor cost rates vary depending on a multitude of factors such as geographic location, part complexity, and market conditions. Labor cost rates must also include benefits, insurance, taxes, and administrative costs. Per the U.S. Bureau of Labor Statistics (BLS), an average of $29.38 of benefits, insurance, and taxes are paid to civilian workers per hour [15]. The median pay for machinists and tool and die makers is $25.57 per hour [16]. An estimated twenty percent overhead is applied to the sum of these rates yields an estimated shop rate of $65.94 per hour.

The starting material cost is influenced by numerous variables, including material type, quality, quantity, supplier, market conditions, and procurement methods. For consistency, all material quotes for this cost analysis were solicited and obtained within the same timeframe (February 2025). For those materials or components that a quote was not provided, a ROM (Rough Order of Magnitude) is denoted. Quotes were requested from reputable vendors and manufacturer recommended distributers. Most NIACS components are machined from 6061-T6 aluminum plate or sheet. For consistency across quotes, a standard stock size of four feet by eight feet was specified.

For those parts that are conventionally machined, manufacturing data exists in the NSROC database. This data includes the issued stock material type, stock material size, lot size, and production time per lot. Using the provided material quotes and the information in the NSROC database, the cost per piece is calculated. When manufacturing data is not provided, a labor estimate is denoted. Manufacturing data for the original NIACS is shown in Table 9.

Item Number	Part Description	Part Quantity	Stock Material Cost	Labor Cost
1.1	Skin	1	$7,598.18	$2,736.51
1.2	Skin Door Doubler[4]	1	$6.09	-
1.3	Skin Door[4]	1	$2.87	-
2.1	Electronics Deck	1	$186.10	$725.34
2.2	GLNMAC Lift Ring	1	$21.00	$23.27
2.3	TERN Angle Bracket	4	$8.71	$226.83
2.4	EFS Mounting Plate	4	$8.16	$61.54
2.5	Frame Top	3	$25.89	$185.95
2.6	GIPS Distribution Frame	1	$16.36	$195.62
2.7	GIPS Regulation Frame	1	$16.36	$191.23
2.8	Driver Board Frame	1	$8.63	$92.32
2.9	GIPS Power Entry Frame	1	$7.92	$151.66
2.1	ACS Flight Processor Frame	1	$11.42	$79.13
2.11	TERN NIACS Connector Plate	1	$1.54	$34.95
3.1	Tank Cradle	2	$54.38	$391.24
3.2	Tank Manifold	2	$9.75	$168.15
3.3	Tank Cushion[4]	4	$1.58	$32.97
3.4	Tank Restraint Clamp[4]	2	$8.73	$13.19
3.5	Spacer Plate	1	$0.80	$13.19
3.6	High Pressure Manifold	1	$7.29	$108.80
3.7	Manifold Spacer	1	$0.27	$13.19
3.8	Bi-Level Transfer Manifold	1	$13.00	$194.52
3.9	Regulator Support Bracket	1	$2.09	$29.31
3.1	Regulator Bracket Spacer	1	$0.16	$2.20
3.11	Main Manifold	1	$18.77	$326.40
3.12	CONX Manifold Bracket, Right	1	$1.22	$24.73
3.13	CONX Manifold Bracket, Left	1	$1.22	$11.54
3.14	Regulator Bracket	1	$2.57	$15.39
4.1	Universal Umbilical Bracket	1	$21.50	$134.52
4.2	Umbilical Backing Plate	1	$0.35	$7.25
5	Deck Mounting Bracket	8	$88.37	$681.38
6	Pneumatic Umbilical	1	$20.16	$276.95
7	Transverse Nozzle Block, Right	2	$19.85	$423.12
8	Transverse Nozzle Block, Left	2	$19.85	$319.81
9	Roll Control Block	2	$59.39	$336.29
10	Transducer Mounting Bracket (1)	2	$0.47	$13.19
11	Transducer Mounting Bracket (2)	1	$0.46	$36.27
12	Main Manifold Mounting Block	1	$3.20	$32.97

Total Material Cost	Total Labor Cost
$8,274.64	$8,310.91

Total Cost	$16,585.55

Table 9: Original NIACS Production Cost

[4] ROM

For the CFRP parts in the composites-based NIACS, labor estimates are required for accurate part and system cost. Both CFRP base materials (T300 3K/934 and MS-1A) are commercially available so the manufacturing process is set by the manufacturer in product data sheets [10] [17]. For BMC-based parts, a mold needs to be fabricated prior to the formation of the part. The abbreviated route sheet for the MS-1A is as follows:

1. Mold Preparation (~ ½ Hour)
2. BMC Measure and Preheat (~ ½ Hour)
3. Cure (~ ½ Hour)
4. Post Cure (~ 2 Hours)
5. Mold Split and Part Ejection (~ ½ Hour)
6. Part Finishing (~ 1 Hour)

While these sequential operations do not require constant monitoring (such as in the case of the curing and post-curing process), labor hour costing will be cumulative. In practice, concurrent operations and production overlap will decrease active labor. In total, five hours are estimated to produce one BMC based part. Based on the quantity of parts required per system or per bath, multiple parts could be formed in one mold. This is accounted for in the composites-based NIACS cost estimate by assuming that one batch accounts for the total quantity of that specific part. For example, four battery standoffs are necessary for a single composites-based NIACS system. Thus, it is assumed that all four parts are formed in the same mold then finished individually. For this part, the labor estimate is as above but part finishing is repeated four times, once per piece.

Like the BMC based parts, a mold or tool is needed for parts formed by stacking the T300 3K/934 prepreg. A similar, abbreviated route sheet for the T300 3K/934 process is below and is for a part of typical size and complexity seen on the NASA sounding rocket program. Like the BMC process, concurrent operations and production overlap will decrease active labor. An autoclave is needed for part curing and depending on the size of the autoclave, multiple parts could be cured concurrently, decreasing part production time.

1. Prepare Consumables (vacuum bag, surface breather, and release films) (~ 1 Hour)
2. Cut Prepreg (~2 Hours)
3. Mold Preparation (~ ½ Hour)
4. Lay-Up and Vacuum Seal Tape (~1 Hour)
5. Cure Cycle (~4 Hours)
6. Part Removal (~ ½ Hour)
7. Part Finishing (~ 1 Hour)

Item Number	Part Description	Part Quantity	Stock Material Cost	Labor Cost
1.1	Skin	1	$6,479.43	$2,637.60
1.2	Skin Door	1	$18.32	$153.86
1.3	Skin Door Doubler	1	$6.09	-
1.3.1	Universal Umbilical Bracket	1	$29.18	$329.70
1.3.2	Umbi Backing Plate	1	$0.35	$7.25
1.4	Deck Mounting Bracket	4	$74.34	$527.52
1.5	Pneumatic Umbilical	1	$29.73	$329.70
1.6	Transverse Nozzle Block, Right	2	$19.85	$423.12
1.7	Transverse Nozzle Block, Left	2	$19.85	$319.81
1.8	Roll Control Block	2	$59.39	$336.29
2.1	Substructure	1	$927.32	$659.40
2.2	Battery Standoff	4	$32.40	$527.52
2.3	Power System Standoff	1	$8.10	$329.70
2.4	Flight Computer Standoff	1	$7.56	$329.70
2.5.1	Frame Top	1	$8.63	$61.98
2.5.2	GIPS Distribution Frame	1	$16.36	$195.62
2.5.3	GIPS Regulation Frame	1	$16.36	$191.23
2.6.1	Frame Top	2	$17.26	$123.97
2.6.2	Driver Board Frame	1	$8.63	$92.32
2.6.3	GIPS Power Entry Frame	1	$7.92	$151.66
2.6.4	ACS Flight Processor Frame	1	$11.42	$79.13
2.7	Substructure Support	1	$952.15	$659.40
2.8	Tank Manifold	2	$9.75	$168.15
2.9	Tank Restraint Clamp	2	$12.44	$13.19
2.1	High Pressure Manifold	1	$7.29	$108.80
2.11	Transducer Standoff	2	$2.52	$395.64
2.12	Bi-Level Transfer Manifold	1	$13.00	$194.52
2.13	Main Manifold	1	$18.77	$326.40
A[5]	Nut Plate	57	$456.00	-

Total Material Cost	Total Labor Cost
$9,280.39	$9,673.18

Total Cost	$18,953.57

Table 10: Composites-Based NIACS Production Cost

[5] ROM

STABILITY ANALYSIS

While reducing payload mass to increase apogee and time above critical altitudes is the primary goal of introducing composite materials to the sounding rocket platform, other vehicle characteristics will be affected. One characteristic of concern is that of launch vehicle stability. Sounding rockets must have positive stability on the upleg trajectory during powered flight. For recovered payloads, the re-entry configuration of the payload must by unstable. This instability is intentional as the payload needs to tumble through Earth's atmosphere on the downleg trajectory to disperse heat across the payload body. Current design practice is to ballast payloads with monolithic materials such as steel and lead at the consequence of vehicle performance.

Reducing payload mass may be negated if ballast is required to maintain launch vehicle stability. To understand the consequences of reducing payload mass, the rigid body stability of all missions conducted by the NSRP in the 2024 fiscal year was conducted. Rigid body stability is primarily a function of the rocket's center of mass and center of lateral area, both of which may be affected by using composite materials. The center of mass will be affected because the payload will contain less mass. The center of lateral area may be affected if the length of payload subsystems is reduced by means of part consolidation and structural redesign, as seen during NIACS reconfiguration. For this rigid body stability analysis, it will be assumed that payload mass is reduced by 19.6% and the center of lateral area is unchanged. In practice, a reduction in payload length will increase rigid body stability because the center of lateral area will shift aft towards the launch vehicle. Thus, the following generalized assessment is conservative.

Rigid body stability for each mission conducted by the NSRP is taken from mission documentation and is given as a minimum rigid static margin (RSM). The RSM is a unitless quantity that, when multiplied by the body diameter of the active stage, gives the linear distance between the center of mass and the center of lateral area (CLA) of the rocket in free motion. A RSM exists for each stage of the sounding rocket except for stages that are used in exo-atmospheric conditions, shown in Table *11*.

Mission Number	1st Stage RSM	2nd Stage RSM	3rd Stage RSM
36.386 UE	4.4	4.1	-
36.387 UE	4.4	4.1	-
36.388 UE	4.4	4.1	-
36.375 UG	4.2	3.6	-
45.007 GE	3.3	2.7	-
52.009 AE	4.4	8.0	3.9
36.392 UE	3.4	2.7	-
36.393 UE	3.4	2.7	-
36.394 UE	3.4	2.7	-
36.370 US	4.5	3.2	-
36.371 NS	4.9	3.8	-
36.396 UG	4.8	4.5	-
41.133 WO	5.0	4.0	-
36.385 NS	4.6	4.1	-
46.042 WO	5.7	2.4	-
36.384 UG	5.1	3.5	-
36.366 US	4.9	3.5	-

Table 11: Baseline Rigid Static Margin Per Stage

The length, mass, and center of mass of each stage and of the payload are known quantities. These quantities will not be disclosed due to the sensitive nature of the information. By summing moments about the theoretical nose tip of the payload (Figure *73*) the position of the CLA can be determined. The RSM of the rocket using a composite based payload is then determined by back calculation. The results as a percentage of RSM are given in Table *12*.

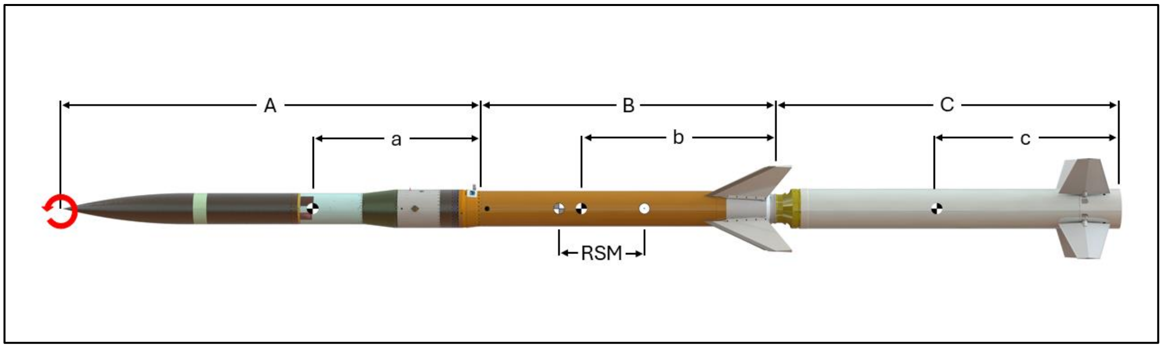

Figure 73: Rigid Static Margin Diagram

Mission Number	1st Stage RSM Delta	2nd Stage RSM Delta	3rd Stage RSM Delta
36.386 UE	-11%	9%	-
36.387 UE	-11%	9%	-
36.388 UE	-11%	9%	-
36.375 UG	-14%	16%	-
45.007 GE	-14%	14%	-
52.009 AE	-6%	-6%	12%
36.392 UE	-10%	10%	-
36.393 UE	-9%	10%	-
36.394 UE	-9%	10%	-
36.370 US	-12%	16%	-
36.371 NS	-12%	14%	-
36.396 UG	-11%	10%	-
41.133 WO	-8%	15%	-
36.385 NS	-10%	10%	-
46.042 WO	-8%	29%	-
36.384 UG	-12%	16%	-
36.366 US	-12%	16%	-

Table 12: Delta Rigid Static Margin Per Stage

In general, a composites-based sounding rocket payload will decrease the first stage RSM by an average of 10% and increase the second stage RSM by 13%, for two-stage vehicles. The four-stage vehicle of 52.009 AE is similar in that the initial stages see a reduction in stability while the later stages see an increase. The decrease in RSM on the first stage is tenable as the programmatic guideline (not given) is met with margin for all missions under consideration. This suggests that if composites-based payloads were to be adopted by the program, additional ballast to compensate for the decrease in payload mass would be unnecessary and that the existing vehicle stable and launch vehicle hardware (fins, interstages, etc.) would be suitable.

Re-entry stability is assessed as a statistical probability of exceeding the re-entry flight envelope, or PERFE. The flight envelope was developed as a cumulative distribution function of the maximum dynamic pressure of the payload body during atmospheric re-entry relative to a subjective heating damage assessment of the payload skins [18]. As the PERFE is dependent on the maximum expected dynamic pressure of the payload re-entry body, and these values cannot be determined from the available information, a generalization is proposed.

It is desirable to decrease the PERFE for all recovered payloads. A decreased PERFE correlates to less heating damage which is necessary from a programmatic and mission cost perspective. The PERFE and dynamic pressure have a positive correlation thus it is desired for a composite-based payload to experience decreased dynamic pressure on the downleg trajectory. The dynamic pressure on an object in a fluid is a function of the fluid mass density and the velocity of the fluid relative to the body, shown in Equation 9.

$$P_d = \frac{1}{2}\rho V^2 \tag{9}$$

The fluid mass density of Earth's atmosphere is independent of payload characteristics so decreasing the velocity of the payload on its downleg trajectory is the only way to decrease dynamic pressure on the payload from a payload design perspective. To decrease the velocity of the payload, the ballistic coefficient of the payload re-entry configuration needs to decrease. The ballistic coefficient is given in Equation 10.

$$C_b = \frac{m}{C_d A} \tag{10}$$

The ballistic coefficient is a function of the body mass, drag coefficient, and cross-sectional area of the body in the freestream flow. A composites-based payload, based on the NIACS reconfiguration, will decrease in both mass and length, therefby decreasing the drag coefficient and cross-sectional area of the payload. As the mass reduction is expected to be greater than the product of the drag coefficient and cross-sectional area, it is reasonable to expect the ballistic coefficient will decrease, thereby decreasing the ballistic velocity of the payload and thus the dynamic pressure.

RESULTS

In order to estimate the impact of adopting composite materials on the NSRP, a standard NSROC subsystem underwent structural reconfiguration using composite materials. The NIACS subsystem was selected as it is representative of sounding rocket payload architecture and contains standard parts within its assembly. The design objective was to minimize the mass of the NIACS without altering its function. The NIACS was deconstructed, and parts were assessed for material change. Based on the NSRP's mission lifecycle and testing philosophy, two CFRP materials were identified as viable alternatives to the commonly used 6061-T6 aluminum in payload design. Material substitutions prompted comprehensive reconfiguration, resulting in a simplified assembly. Structural CFRP parts underwent design-analysis via FEA to demonstrate each part will withstand the loading environment of a NASA sounding rocket payload. The reconfigured NIACS yielded a mass reduction of $13.37\ lb_m$, or 19.6%, relative to the original subsystem. The reconfigured NIACS is three inches shorter and contains 33% few parts.

As the NIACS is representative of NASA sounding rocket payload architecture, the mass reduction seen in the NIACS was applied to payloads in entirety for missions conducted by the NSRP in the 2024 fiscal year. A year of missions was selected as it represents a variety of experiment categories, launch vehicle types, and launch range locations. Using the mission manifest as a baseline of comparison, the apogee and time above the Kármán Line for composites-based payloads were estimated using published carpet plots of sounding rocket launch vehicles. On average, each mission launched in fiscal year 2024 gained 59.8 kilometers in apogee and 62.9 seconds above the Kármán Line, an increase of 19.2% and 14.8% respectively.

While significant, the benefit to individual missions is dependent on that mission's success criteria. Table 13 shows each mission launched in fiscal year 2024 and summarizes apogee and time above altitude success criteria. A subjective assessment of whether the mission would have benefitted from having additional time above an altitude or reaching a minimum apogee is noted.

Mission Number	Minimum Apogee	Time Above	Beneficial
36.386 UE	325 km	-	No
36.387 UE	325 km	-	No
36.388 UE	325 km	-	No
36.375 UG	-	300 s above 130 km	Yes
45.007 GE	325 km	-	Yes
52.009 AE	-	100 s above 300 km	Yes
36.392 UE	375 km	-	No
36.393 UE	375 km	-	No
36.394 UE	375 km	-	No
36.370 US	-	300 s above 150 km	Yes
36.371 NS	-	290 s above 150 km	Yes
36.396 UG	-	215 s above 250 km	Yes
41.133 WO	N/A	N/A	No
36.385 NS	N/A	300 s above 150 km	Yes
46.042 WO	N/A	N/A	No
36.384 UG	-	360 s above 100 km	Yes
36.366 US	-	260 s above 160 km	Yes

Table 13: Mission Benefit

Of the missions launched in fiscal year 2024, nine would have benefitted from a composites-based payload. Of these nine, seven are either optical astrophysics or heliophysics investigations. These are telescope borne payloads that benefit from additional observation time during their trajectory. For this class of mission (typically launched on the Black Brant IX), an average of 60.3 seconds of additional time above the Kármán Line would have been possible. This additional observation time may allow an additional target to be observed per flight or for additional observation of a single target to be taken on a single flight. The other two missions in fiscal year 2024 that would have benefitted are geospace sciences investigations (45.007 UE and 52.009 AE) that had mission success criteria either to reach a minimum apogee of 325 km or 100 s above 300 km. These missions had substantial payload mass ($1{,}065.6\ lb_m$ and $967.6\ lb_m$) that warranted a higher impulse launch vehicle to meet their success criteria. A proposed benefit of incorporating composite materials on NSRP payloads is enabling lower-impulse, military surplus launch vehicles to achieve apogees comparable to those of higher-impulse commercial alternatives. For mission 45.007 GE, if the payload had been designed with composite materials, it may have been able to use a Black Brant IX launch vehicle. Referencing the carpet plot for the Black Brant IX, the composite based payload would have reached an apogee of ~358 km. When considering the same for mission 52.009 AE, there is not enough information in the carpet plots to definitely assess whether decreasing the payload mass would have allowed a lower impulse launch vehicle to be used. Subjectively, 52.009 AE may have been able to utilize a three-stage, Black Brant XI-A. Of all missions launched in fiscal year 2024, only these two missions could have utilized a different, lower impulse, launch vehicle. Considering missions 41.133 WO and 46.042 WO, these are student missions so the increase in payload performance metrics do not benefit these missions so conventional materials should remain the predominant material.

Considering NIACS production cost, to implement composite materials would incur a 12% increase in material and 16% increase in labor costs, or 14% overall. The implementation cost for composite materials in the NIACS subsystem is disproportionately influenced by the skin forging cost, which constitute the majority of raw material costs (92% in the original NIACS). By reducing the NIACS skin length through structural reconfiguration of the internal subassembly, most of the CFRP material costs are offset. If the cost of the skin material is not considered, production costs increase by 39%.

CONCLUSION

It is evident that composite material adoption by the NASA Sounding Rocket Program will increase the apogee and time above the Kármán Line for individual missions. This study demonstrates the potential for a 19.6% payload mass reduction if composite materials are implemented on the payload scale. This results in an average apogee increase of 59.8 kilometers and 62.9 seconds above the Kármán Line per mission on an annualized basis. A majority of missions launched in the 2024 fiscal year would have benefitted from composite material use, especially optical astrophysics and heliophysics mission types. Only two missions could have used a lower impulse launch vehicle to achieve mission success if the payloads were designed using composite materials.

Composite material adoption will incur additional production costs on the program, on the order of 39%, unless implementation is coupled with part quantity and skin length reduction. For example, NIACS reconfiguration resulted in the skin length decrease of three inches and part quantity decrease of 33%. These reductions limited the production cost increase to 14% overall.

Given the program's diverse mission manifest, widespread adoption of composite materials is not advised. While beneficial for some missions, the increased manufacturing costs do not justify universal adoption across all payloads. However, as all optical astrophysics and heliophysics missions benefitted from the additional time above the Kármán Line for their investigations, it is recommended that subsystems common to this mission type are redesigned using composite materials. Such subsystems include the SPARCS (Solar Pointing Attitude Rocket Control System), CACS (Celestial Attitude Control System), Shutter Door, and NFORSe (NSROC Forward Ogive Recovery System). Generally, any system that commonly launches on either optical astrophysics or heliophysics mission and is recovered should be considered for update. Due to the increased production costs, composite material-based parts should be internal to the payload with the intent to refurbish and launch multiple times to decrease lifecycle costs.

REFERENCES

[1] Burth et al., "NASA Sounding Rockets User Handbook," NASA/TP-20230006855, May 2023.

[2] Pfaff et al., "Findings & Concerns, Meeting of June 9, 2000, Sounding Rocket Working Group, National Aeronautics and Space Administration," June 2000. https://rscience.gsfc.nasa.gov/mt_00_jun_find.html

[3] Kaiser et al., "Report of the SRWG Sub-committee on High Altitude Rockets to Increase Astrophysics and Solar Observing Time," October 2009. https://rscience.gsfc.nasa.gov/keydocs.html

[4] Pfaff et al., "Sounding Rocket Working Group, National Aeronautics and Space Administration, Meeting of February 5, 2019, Findings,", February 2019. https://rscience.gsfc.nasa.gov/srwg.html

[5] Zenten, F., and Backer, W., "Composite Sounding Rocket Payloads: A Structural Design Study," October 2022.

[6] "NASA Sounding Rockets Bluebook," February 2025. https://sites.wff.nasa.gov/code810/files/BlueBook.pdf

[7] "B.9 Heliophysics Low Cost Access to Space," NNH23ZDA001N-HLCAS, February 2023. https://nspires.nasaprs.com/external/solicitations/summary!init.do?solId={CBAAE9AA-8E58-1FCD-CACE-3120FBA5FB0F}&path=open

[8] Kaw, A. K., "Mechanics of Composite Materials," *2nd ed.,* CRC Press, Florida, 2006, pp. 19-29.

[9] "Composite Materials Handbook," *Polymer Matrix Composites: Materials Properties*, 17 ed., Vol. 2, Rev. H, Part B, SAE International, 2018, pp. 2B-186-2B-197

[10] "Toray MS-1A," *Product Data Sheet* https://www.toraytac.com/media

[11] Highsmith, A., "Post-Impact Behavior of Composite Solid Rocket Motor Cases", 1992

[12] Zemann, R., "Manufacturing of Threads Direct into a Carbon Fibre Reinforced Polymer," *Materials Today: Proceedings*, Vol. 1, Issue 4, 2016 https://www.sciencedirect.com/science/article/pii/S2214785316002066

[13] "Load Analyses of Spacecraft and Payloads," NASA-STD-5002A, NASA, September 2019.

[14] Dieter, G.E., "Engineering Design," *5th ed.*, McGraw-Hill, New York, 2013, pp. 781-792

[15] "Employer Costs per Hour Worked for Employee Benefits," December 2019. https://www.bls.gov/charts/employer-costs-for-employee-compensation/benefits-per-hour.htm

[16] "Occupational Outlook Handbook," *Machinists and Tool and Die Makers*. 2023. https://www.bls.gov/ooh/production/machinists-and-tool-and-die-makers.htm#tab-1

[17] "CYCOM® 934 Epoxy Prepreg," *Technical Data Sheet* https://www.heatcon.com/wp-content/uploads/2015/08/HCS2402-060-Cytec-Carbon-Fiber-Prepreg-Cycom-934-PX-T300-ST.pdf

[18] Lanzi, R., and Vincent, B., "Development and Application of an Empirical Probability Distribution for the Prediction Error of Re-Entry Body Maximum Dynamic Pressure"

VITA

Robert Henry Burth

Old Dominion University
Mechanical & Aerospace Engineering

241 Kaufman Hall
Norfolk, VA 23529

2016	Bachelor of Science in Mechanical Engineering, Clemson University
2017 - 2018	Associate Mechanical Engineer, Hawk Institute for Space Sciences, LLC
2018 - 2020	Launcher Systems Engineer, Northrop Grumman
2020 – 2021	Mechanical Engineer, Northrop Grumman
2021 - 2022	Mechanical Engineer, Peraton
2022 - 2024	Mission Manager, Peraton
2024 - Present	Technical Task Lead, Peraton

LICENSES AND CERTIFICATIONS
Engineer in Training, Maryland Department of Labor (ID# 57409)
Project Management Professional (#3783331)

PUBLICATIONS
Burth et al., “NASA Sounding Rockets User Handbook,” NASA/TP-20230006855, May 2023.